

# Ca<sup>2+</sup> and K<sup>+</sup> channels of normal human adrenal zona fasciculata cells: Properties and modulation by ACTH and AngII

John J. Enyeart and Judith A. Enyeart

Department of Neuroscience, The Ohio State University Wexner Medical Center, Columbus, OH 43210

In whole cell patch clamp recordings, we found that normal human adrenal zona fasciculata (AZF) cells express voltage-gated, rapidly inactivating Ca<sup>2+</sup> and K<sup>+</sup> currents and a noninactivating, leak-type K<sup>+</sup> current. Characterization of these currents with respect to voltage-dependent gating and kinetic properties, pharmacology, and modulation by the peptide hormones adrenocorticotrophic hormone (ACTH) and AngII, in conjunction with Northern blot analysis, identified these channels as Ca<sub>v</sub>3.2 (encoded by CACNA1H), Kv1.4 (KCNA4), and TREK-1 (KCNK2). In particular, the low voltage-activated, rapidly inactivating and slowly deactivating Ca<sup>2+</sup> current (Ca<sub>v</sub>3.2) was potently blocked by Ni<sup>2+</sup> with an IC<sub>50</sub> of 3 μM. The voltage-gated, rapidly inactivating K<sup>+</sup> current (Kv1.4) was robustly expressed in nearly every cell, with a current density of 95.0 ± 7.2 pA/pF (*n* = 64). The noninactivating, outwardly rectifying K<sup>+</sup> current (TREK-1) grew to a stable maximum over a period of minutes when recording at a holding potential of -80 mV. This noninactivating K<sup>+</sup> current was markedly activated by cinnamyl 1-3,4-dihydroxy-α-cyanocinnamate (CDC) and arachidonic acid (AA) and inhibited almost completely by forskolin, properties which are specific to TREK-1 among the K2P family of K<sup>+</sup> channels. The activation of TREK-1 by AA and inhibition by forskolin were closely linked to membrane hyperpolarization and depolarization, respectively. ACTH and AngII selectively inhibited the noninactivating K<sup>+</sup> current in human AZF cells at concentrations that stimulated cortisol secretion. Accordingly, mibefradil and CDC at concentrations that, respectively, blocked Ca<sub>v</sub>3.2 and activated TREK-1, each inhibited both ACTH- and AngII-stimulated cortisol secretion. These results characterize the major Ca<sup>2+</sup> and K<sup>+</sup> channels expressed by normal human AZF cells and identify TREK-1 as the primary leak-type channel involved in establishing the membrane potential. These findings also suggest a model for cortisol secretion in human AZF cells wherein ACTH and AngII receptor activation is coupled to membrane depolarization and the activation of Ca<sub>v</sub>3.2 channels through inhibition of hTREK-1.

## INTRODUCTION

In mammals, adrenal zona fasciculata (AZF) cells of the adrenal cortex secrete glucocorticoids in a diurnal pattern in response to stimulation by adrenocorticotrophic hormone (ACTH). Superimposed on this basal secretory pattern, physical and psychological stress triggers bursts of ACTH-stimulated cortisol production by activation of the hypothalamic pituitary adrenal axis (Stewart and Krone, 2011). In some species, including bovine and human, AngII may also stimulate cortisol secretion (Clyne et al., 1993; Lebrethon et al., 1994; Mlinar et al., 1995). Cortisol acts pivotally in regulating physiological functions ranging from energy metabolism to long-term memory formation (Stewart and Krone, 2011; Chen et al., 2012). At the cellular level, the biochemical and ionic mechanisms that regulate glucocorticoid production are only partially understood. However, in bovine and rodents, a pivotal role for depolarization-dependent Ca<sup>2+</sup> entry is well established (Matthews and Saffran, 1973; Lymangrover et al., 1982;

Enyeart et al., 1993; Mlinar et al., 1993a,b; Barbara and Takeda, 1995). In this regard, relatively few studies exist describing the specific ion channels of normal mammalian AZF cells, including their modulation by ACTH and AngII.

Early intracellular recordings from cat, rabbit, bovine, rat, and mouse adrenocortical tissue and isolated AZF cells showed that they maintained negative resting potentials, determined primarily by the membrane permeability to K<sup>+</sup> (Matthews, 1967; Matthews and Saffran, 1968, 1973; Natke and Kabela, 1979; Lymangrover et al., 1982; Quinn et al., 1987). In addition, ACTH was found to depolarize mouse and rabbit AZF cells and, in some cases, to induce action potential-like spikes in these cells (Matthews and Saffran, 1968, 1973; Lymangrover et al., 1982). Ca<sup>2+</sup>-dependent action potential-like waveforms have also been recorded in cat, rat, and bovine AZF cells in response to application of depolarizing current (Natke and Kabela, 1979; Quinn et al.,

Correspondence to John J. Enyeart: enyeart.1@osu.edu

Abbreviations used in this paper: AA, arachidonic acid; ACTH, adrenocorticotrophic hormone; AZF, adrenal zona fasciculata; AZG, adrenal zona glomerulosa; CDC, cinnamyl 1-3,4-dihydroxy-α-cyanocinnamate; II-V, instantaneous I-V.

© 2013 Enyeart and Enyeart. This article is distributed under the terms of an Attribution-Noncommercial-Share Alike-No Mirror Sites license for the first six months after the publication date (see <http://www.rupress.org/terms>). After six months it is available under a Creative Commons License (Attribution-Noncommercial-Share Alike 3.0 Unported license, as described at <http://creativecommons.org/licenses/by-nc-sa/3.0/>).

1987; Barbara and Takeda, 1995). Most of the action potentials observed in AZF cells were obtained in recordings from intact tissue rather than isolated cells. Recently, spontaneous action potential-like oscillations have been observed in a mouse adrenal zona glomerulosa (AZG) slice preparation (Hu et al., 2012). Overall, these studies suggested a critical role for ion channels and voltage-dependent  $\text{Ca}^{2+}$  channels in ACTH-stimulated cortisol secretion.

Later studies that combined patch clamp and molecular cloning techniques identified each of the ion channels expressed by bovine AZF cells and described their modulation by ACTH and AngII. Specifically, bovine AZF cells were found to express voltage-gated, rapidly inactivating  $\text{Ca}_v3.2$   $\text{Ca}^{2+}$  and  $\text{Kv}1.4$   $\text{K}^+$  channels and a novel leak-type  $\text{K}^+$  channel that set the resting membrane potential (Mlinar and Enyeart, 1993b; Mlinar et al., 1993 a,b). This leak-type  $\text{K}^+$  channel, later identified as TREK-1 of the two-pore  $\text{K}^+$  (K2P) channel family, was potently inhibited by ACTH and AngII, leading directly to membrane depolarization (Mlinar et al., 1993a; Enyeart et al., 2002). These findings led us to propose a model for cortisol secretion in which ACTH or AngII receptor activation was coupled to membrane depolarization and the activation of  $\text{Ca}_v3.2$  channels through the inhibition of TREK-1 channels (Enyeart et al., 1993, 2005; Mlinar et al., 1993a; Liu et al., 2008).

The molecular identities of ion channels expressed in AZF cells, other than bovine, haven't been determined. Therefore, it isn't known to what extent mammalian AZF cells resemble each other with respect to their ion channels and associated electrical properties. In particular, it isn't known whether these cells all express a similar group of channels, including a K2P channel that sets the resting membrane potential and whose inhibition by ACTH or AngII is tightly linked to membrane depolarization. In one patch clamp study, rat AZF cells were found to express only a relatively  $\text{Ni}^{2+}$ -insensitive T-type  $\text{Ca}^{2+}$  current and a slowly inactivating A-type  $\text{K}^+$  current, whereas no leak-type  $\text{K}^+$  current was detected (Barbara and Takeda, 1995). By comparison, in the mouse adrenocortical Y-1 cell line, only two types of voltage-gated  $\text{Ca}^{2+}$  currents and a  $\text{Ca}^{2+}$ -activated  $\text{K}^+$  current were detectable (Tabares et al., 1985).

Recordings from bovine, rat, and mouse adrenocortical cells suggest that considerable variability may exist among mammalian AZF cells with respect to the ion channels and electrical events that mediate corticosteroid secretion. To understand the role of specific ion channels in secretion by human AZF cells, it will be necessary to identify these channels, including their modulation by peptide hormones that regulate cortisol production. In the present study, we have identified and characterized the ionic currents of normal human AZF cells with respect to their biophysical properties, pharmacology, and modulation by ACTH and AngII.

## MATERIALS AND METHODS

### Materials

Tissue culture media, antibiotics, fibronectin, and FBS were obtained from Invitrogen. Coverslips were purchased from Bellco. PBS, 1,2 *bis*-(2-aminophenoxy)ethane-*N,N,N',N'*-tetraacetic acid (BAPTA), MgATP, collagenase (C0130), DNase, forskolin, ACTH (1–24), AngII,  $\text{GdCl}_3$ ,  $\text{NiCl}_2$ , mibefradil, and arachidonic acid (AA) were obtained from Sigma-Aldrich. Cinnamyl 1-3,4-dihydroxy- $\alpha$ -cyanocinnamate (CDC) was purchased from Enzo Life Sciences. hTASK-3 (KCNK9 cDNA clone) was purchased from Thermo Fisher Scientific (MGC:103976 IMAGE:30915383).  $\alpha$ -[ $^{32}\text{P}$ ]dCTP was purchased from PerkinElmer.

### Isolation and culture of AZF cells

Human adrenals were obtained from 11 deceased organ donors (age 10–62 yr, male and female, of either Caucasian or African-American race) through the Ohio State University Department of Transplant Surgery and Lifeline of Ohio within 3 h of organ removal from the donor. Institutional Review Board and ethical consenting practices for donor tissue were strictly followed. Organs were kept in cold saline, on wet ice until they were available to be collected. Some adrenal cell isolations (3/11) yielded cells that could not be used for our experiments, as indicated by extremely fragile membranes and lack of recordable ion currents. We were not able to ascertain whether this was caused by our cell isolation protocol or the treatment of the organs after harvest before we received them. This characteristic was not related to age, sex, or race of the donor. However, we were able to develop a method for isolating and storing human AZF cells from a majority of the glands received (8/11) wherein they retained their biochemical and electrophysiological properties for a minimum of 18 mo. In brief, glands with some surrounding fat were submerged in cold PBS, kept on ice, and transported within 3 h of removal from the donor to the laboratory. Fat was removed, and thin tissue slices were obtained using a Stadie-Riggs tissue slicer. The first slice containing mainly adrenal capsule and zona glomerulosa was used for the isolation of adrenal glomerulosa cells. Subsequent slices were designated as fasciculata and were used to prepare AZF cells. In 7 of 11 isolations, the adrenal medulla could be easily identified and manually dissected away from the cortex. In the remaining cases, the medulla, as observed under a dissecting microscope, appeared to infiltrate the cortex and was thus more difficult to separate from the outer layers of the adrenal cortex. This characteristic was not related to age, sex, or race of the donor. Cortical slices were finely chopped into 1–2-mm fragments, followed by two incubation periods of 60 min in 2 mg/ml DMEM/F12-containing collagenase (C0140; Sigma-Aldrich) and 0.5 mg/ml DNase (DN25; Sigma-Aldrich). Cells were then disrupted by gentle aspiration with a sterile, fire-polished Pasteur pipette before being filtered using a cell dissociation sieve (#60 mesh; CD-1; Sigma-Aldrich) and centrifuged for 5 min at 100 *g*. The cell pellet was washed twice with DMEM/F12, resuspended in DMEM/F12 (1:1), 10% FBS, 100 U/ml penicillin, 0.1 mg/ml streptomycin, 1  $\mu\text{M}$  of antioxidant  $\alpha$ -tocopherol, 20 nM selenite, and 100  $\mu\text{M}$  ascorbic acid (DMEM/F12 $^+$ ) and either plated for immediate use or resuspended in FBS/5% DMSO, divided into 1-ml aliquots, and frozen (initially at  $-80^\circ\text{C}$  for 24 h and then at approximately  $-196^\circ\text{C}$  in a Thermolyne Locator Plus liquid nitrogen canister) for future use. Frozen cells were found to be viable when thawed, after storage for as long as 18 mo, with no change in measurable  $\text{K}^+$  or  $\text{Ca}^{2+}$  currents. To ensure cell attachment when culturing cells, glass coverslips (9 × 9 mm; Bellco) in 35-mm dishes were treated with 10  $\mu\text{g}/\text{ml}$  fibronectin at  $37^\circ\text{C}$  for 30 min and then rinsed with warm, sterile PBS immediately before adding cells. Cells were maintained at  $37^\circ\text{C}$  in a humidified atmosphere of 95% air–5%  $\text{CO}_2$ .

### Measurement of ion channel mRNA

RNeasy columns (QIAGEN) that had been treated with RNase-free DNase (QIAGEN) to remove genomic contamination were used to extract total RNA from hAZF cells that had been isolated and cultured in DMEM/F12<sup>+</sup> as described above for 24 h. 10 µg of total RNA/lane was separated on an 8% formaldehyde, 1.0% agarose gel and then transferred to a nylon membrane (Gene Screen Plus, NEN). RNA was fixed to the membrane by UV cross-linking. Northern blots were prehybridized for 2 h at 42°C in ULTRAhyb (Ambion), hybridized with each α-[<sup>32</sup>P]dCTP-labeled probe for 18 h, and washed as previously described (Enyeart et al., 2003). Specific probes were as follows: 800 bp CACNA1H probe, which codes for the Ca<sub>v</sub>3.2 channel, was as previously described (Liu et al., 2010; J.A. Enyeart et al., 2011); 1.3-kb PVUII fragment for the KCNA4 probe (coding for the Kv1.4 K<sup>+</sup> channel) was obtained as previously described (Enyeart et al., 2000); 700 bp KCNK2 probe for the TREK-1 channel was obtained by ECOR1 digest of the full-length KCNK2 cDNA as previously described (Enyeart et al., 2002); and full-length KCNK9 probe for the TASK-3 channel was obtained from EcoRI digest of purchased KCNK9 cDNA clone (MGC:103976 IMAGE:30915383; Thermo Fisher Scientific). Northern autoradiograms were imaged using a Typhoon 9200 variable mode phosphorimager after 4-h exposure to phosphorimaging screen (GE Healthcare).

### Patch clamp experiments

**Cellular identification for patch clamp experiments.** Precautions were taken to ensure that the cells selected for recording were AZF cells. First, within the AZF fraction, we selected larger cells (C<sub>p</sub> = 15–30 pF) because AZG cells are typically smaller with capacitance < 15 pF. Second, in whole cell patch voltage clamp recordings, we found that human AZG cells expressed a distinctive inwardly rectifying K<sup>+</sup> current that was not present in AZF cells. This current resembled the KCNJ5 K<sup>+</sup> current recently reported to be selectively expressed in the zona glomerulosa of the human adrenal gland (Choi et al., 2011). Furthermore, the Ca<sup>2+</sup> current that we identified in human AZF cells differs markedly from those previously described in a study of human AZG ion currents (Payet et al., 1994). Presumed AZG cells expressing an inwardly rectifying current were not included in the present study. A few adrenal chromaffin cells were occasionally present in the human AZF fraction. These were easily distinguished by their distinct appearance and the presence of a TTX-sensitive Na<sup>+</sup> current.

**Ca<sup>2+</sup> currents.** Patch clamp recordings of Ca<sup>2+</sup> channel currents were made in the whole cell configuration from human AZF cells. The standard pipette solution was 120 mM CsCl, 1 mM CaCl<sub>2</sub>, 2 mM MgCl<sub>2</sub>, 11 mM BAPTA, 10 mM HEPES, and 1 mM MgATP, with pH titrated to 7.2 with CsOH. The external solution consisted of 117 mM tetraethylammonium chloride, 5 mM CsCl, 10 mM CaCl<sub>2</sub>, 2 mM MgCl<sub>2</sub>, 5 mM HEPES, and 5 mM glucose, with pH adjusted to 7.4 with tetraethylammonium hydroxide.

**K<sup>+</sup> currents.** Patch clamp recordings of K<sup>+</sup> channel currents were made in the whole cell configuration from human AZF cells. The standard external solution consisted of 141.5 mM NaCl, 5 mM KCl, 1 mM CaCl<sub>2</sub>, 2 mM MgCl<sub>2</sub>, 10 mM HEPES, and 5 mM glucose, with pH adjusted to 7.3 using NaOH. The standard pipette solution consisted of 120 mM KCl, 1 mM CaCl<sub>2</sub>, 2 mM MgCl<sub>2</sub>, 11 mM BAPTA, 10 mM HEPES, 5 mM ATP, and 200 µM GTP, with pH titrated to 6.8–7.2 using KOH. All solutions were filtered through 0.22-µm cellulose acetate filters.

### Recording conditions and electronics

AZF cells were used for patch clamp experiments 2–48 h after plating. Typically, cells with diameters of 15–30 µm and capacitances

of 15–30 pF were selected. Coverslips were transferred from 35-mm culture dishes to the recording chamber (volume: 1.5 ml) that was continuously perfused by gravity at a rate of 3–5 ml/min. For whole cell recordings, patch electrodes with resistances of 1.0–2.0 MΩ were fabricated from Corning 0010 glass (World Precision Instruments). These electrodes routinely yielded access resistances of 1.5–4.0 MΩ and voltage clamp time constants of <100 µs. K<sup>+</sup> and Ca<sup>2+</sup> currents were recorded at room temperature (22–25°C) according to the procedure of Hamill et al. (1981) using a List EPC-7 patch clamp amplifier. To minimize series resistance errors, smaller cells (15–20 pF) and lower resistance electrodes (<1.5 MΩ) were chosen for measurement of voltage-dependent gating and kinetic properties. Currents in these cells were not qualitatively different from those in larger cells.

Pulse generation and data acquisition were performed using a personal computer and PCLAMP software with Digidata 1200 interface (Axon Instruments, Inc.). Currents were digitized at 2–50 KHz after filtering with an 8-pole Bessel filter (Frequency Devices). Linear leak and capacity currents were subtracted from current records using summed scaled hyperpolarizing steps of 1/3 to 1/4 pulse amplitude. Data were analyzed using CLAMPFIT 9.2 (Molecular Devices) and SigmaPlot (version 11.0) software. Drugs were applied by bath perfusion, controlled manually by a six-way rotary valve.

### Cortisol assay

In experiments measuring cortisol secretion, human AZF cells were plated in fibronectin-coated 35-mm dishes at a density of 0.2–0.4 million cells per dish in DMEM/F12<sup>+</sup>. After a recovery period of 4 h, media were changed to defined media consisting of DMEM/F12 with 50 µg/ml, 100 U/ml penicillin, and 0.1 mg/ml streptomycin (DMEM/F12/BSA/pen-strep). Cells were maintained in DMEM/F12/BSA/pen-strep for an additional 48 h before changing to the same media either with or without ACTH and/or AngII for the required times. Media from experiments were either assayed immediately after collection or frozen (–20°C) until all samples were collected. All assay conditions were performed in triplicate. Cortisol secretion by AZF cells was measured using a Cortisol EIA kit (11-CORHU-E01; Alpco Immunoassays) according to the manufacturer's directions. If necessary, media samples were diluted using DMEM/F12/BSA/pen-strep media.

## RESULTS

### Voltage-gated Ca<sup>2+</sup> currents

In whole cell patch clamp recordings, we found that human AZF cells expressed only a low voltage-activated, rapidly inactivating Ca<sup>2+</sup> current resembling T-type Ca<sup>2+</sup> currents carried through Ca<sub>v</sub>3 channels (Perez-Reyes, 2003). The current-voltage (I-V) relationship for Ca<sup>2+</sup> currents was obtained by applying voltage steps to various test potentials from a holding potential of –80 mV. Ca<sup>2+</sup> currents were measurable at test voltages positive to –50 mV, reached a maximum amplitude between –30 and –10 mV, and declined thereafter, reversing near 50 mV (Fig. 1 A). At test voltages positive to –40 mV, the Ca<sup>2+</sup> current decayed to near zero during a 300-ms depolarization. In 14 similar experiments, in which I-V relationships were obtained, only a low voltage-activated, rapidly inactivating Ca<sup>2+</sup> current with mean maximum density of 15.8 ± 1.9 pA/pF (*n* = 15) was present. A noninactivating Ca<sup>2+</sup> current was not detected in any of these cells.

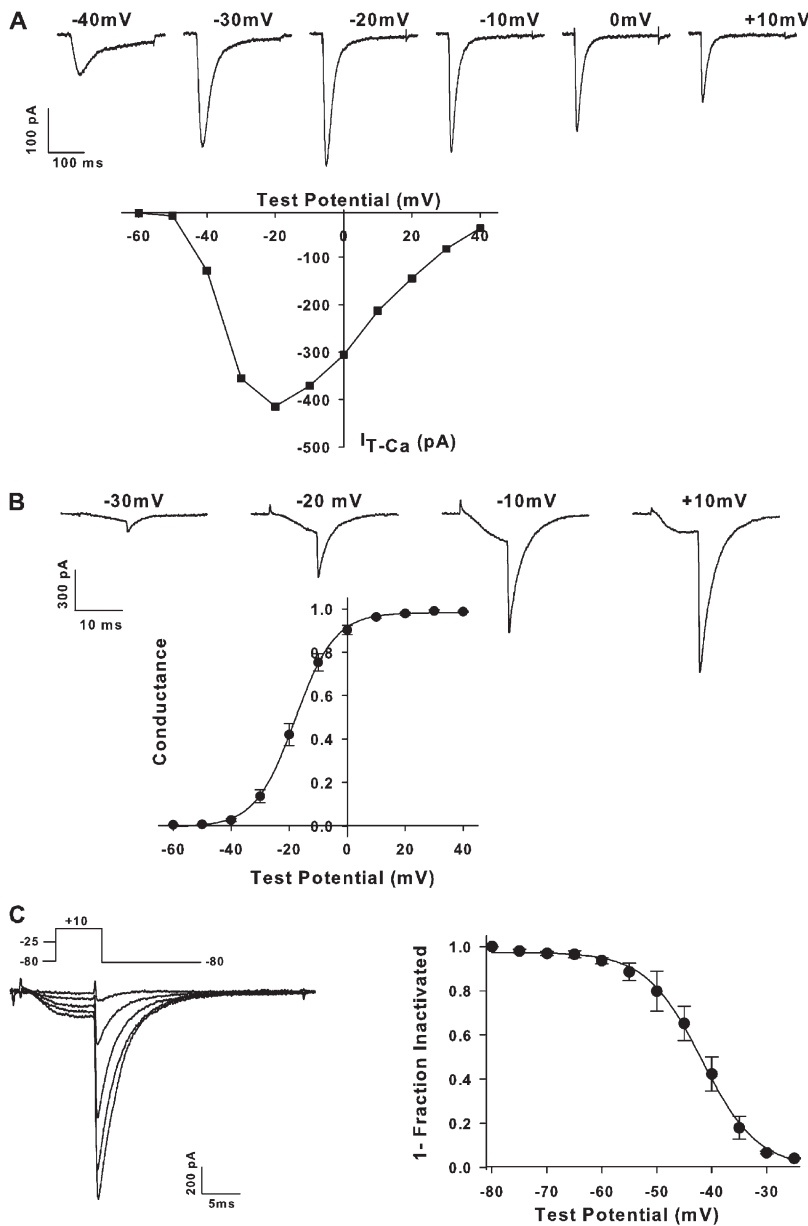


**Figure 1.** T-type  $Ca^{2+}$  current in human AZF cells. The voltage-dependent gating including activation and steady-state inactivation of  $Ca^{2+}$  currents was studied in whole cell patch clamp recordings from human AZF cells. (A) I-V relationship:  $Ca^{2+}$  currents were activated by voltage steps to various test potentials applied at 30-s intervals from a holding potential of  $-80$  mV. Current traces were recorded at the indicated test potentials, and peak current amplitudes were plotted against test voltage. (B) Voltage-dependent activation: 10-ms voltage steps were applied at 30-s intervals from a holding potential of  $-80$  mV before returning to  $-80$  mV where tail currents were measured. Normalized current amplitudes (mean values  $\pm$  SEM) from eight cells were plotted against voltage and fit by a Boltzmann function of the form  $G = 1 / [1 + \exp((v_{1/2} - v) / k)]$ , where  $v_{1/2}$  is the voltage of half maximal conductance and  $k$  is the slope factor. (C) Voltage-dependent steady-state inactivation: Currents were activated by 10-ms test pulses to  $10$  mV after 10-s conditioning steps to potentials between  $-80$  and  $-25$  mV. Peak tail current amplitudes, normalized to the maximum current recorded at  $-80$  mV, were plotted against conditioning voltage. Mean values  $\pm$  SEM ( $n = 4$ ) were fitted with a Boltzmann relationship:  $I / I_{MAX} = 1 / [1 + \exp((v - v_{1/2}) / k)]$ , where  $v_{1/2}$  is the voltage at which half of the channels were inactivated and  $k$  is the slope factor.

**Voltage-dependent activation of  $Ca^{2+}$  channels.** Voltage-dependent opening at relatively negative potentials is a distinctive feature of all three  $Ca_v3$  channel subtypes (Perez-Reyes, 2003). The voltage-dependent activation of  $Ca^{2+}$  channels in human AZF cells was studied by applying voltage steps to various test potentials and measuring the peak  $Ca^{2+}$  tail current upon repolarization to  $-80$  mV (Fig. 1 B). Current amplitudes were normalized, plotted as a fraction of maximal conductance against test voltage, and fit by a Boltzmann function of the form  $G = 1 / [1 + \exp((v_{1/2} - v) / k)]$ , where  $G$  is the relative conductance,  $v_{1/2}$  is the voltage of half-maximal conductance, and  $k$  is the slope factor. Averaged data from eight cells were well fit by a Boltzmann function with a  $v_{1/2}$  of  $-20.19 \pm 0.66$  mV and a slope factor of  $6.67 \pm 0.59$  (Fig. 1 B).

**Voltage-dependent steady-state inactivation.** The voltage dependence of steady-state inactivation of the  $Ca^{2+}$  current was measured by applying 10-s depolarizing pulses to various potentials between  $-80$  and  $-25$  mV, followed by short activating steps to  $10$  mV. Normalized tail currents measured at  $-80$  mV were averaged from four cells, plotted as a function of conditioning voltage, and fit with an equation of the form  $I / I_{MAX} = 1 / [1 + \exp((v - v_{1/2}) / k)]$ , where  $I_{MAX}$  was the current activated from a holding potential of  $-80$  mV. Inactivation was a steep function of voltage with a  $v_{1/2}$  of  $-43.5 \pm 1.70$  mV and a slope factor  $k$  of  $-5.17 \pm 1.32$  mV per  $e$ -fold change (Fig. 1 C).

**Voltage-dependent gating kinetics.** Although the voltage-dependent gating, including activation and steady-state inactivation, is similar among the three  $Ca_v3$  subtypes, their

gating kinetics display significant variability (Klößner et al., 1999; Perez-Reyes, 2003). The expression of only voltage-gated T-type  $\text{Ca}^{2+}$  channels by the great majority of human AZF cells allowed their voltage-dependent kinetic properties to be studied in isolation over a wide range of test potentials.

The activation kinetics of the human  $\text{Ca}^{2+}$  current was voltage dependent, accelerated at positive potentials, and marked by a clear delay in onset. To describe the sigmoidal current, traces were fit with an equation of the form  $I_{\text{Ca}} = I_{\infty} [1 - \exp(-T / \tau_a)]^N \exp(-T / \tau_i)$ , where  $\tau_a$  and  $\tau_i$  are activation and inactivation time constants and  $N$  is an integer between 1 and 4. Best fits were obtained with  $N$  fixed at 4. The activation time constant ( $\tau_a$ ) varied from  $2.39 \pm 0.12$  ms to  $0.50 \pm 0.08$  ms ( $n = 21$ ) at test voltages of  $-30$  mV and  $40$  mV, respectively. The relationship between  $\tau_a$  and voltage could be fit with a single exponential that included an  $e$ -fold change per  $42.4 \pm 3.41$  mV (Fig. 2 A).

Human AZF cell T current inactivation kinetics was also voltage dependent, accelerated by stronger depolarizations, and reached a clear voltage-independent minimum. The inactivating component of T-type currents, recorded as described in the legend of Fig. 1 A at test voltages between  $-40$  and  $40$  mV, was fit with a single exponential function. For test potentials ranging from  $-40$  to  $\sim 0$  mV,  $\tau_i$  decreased smoothly with voltage until, at potentials between  $0$  and  $40$  mV,  $\tau_i$  approached a distinct voltage-independent minimum value (Fig. 2 B). The relationship expressing  $\tau_i$  as a function of voltage could be fit by a single exponent with an  $e$ -fold change per  $9.47 \pm 1.15$  mV ( $n = 11$ ) and a voltage-independent offset of  $18.31 \pm 1.68$  ms.

Among all  $\text{Ca}^{2+}$  channel subtypes,  $\text{Ca}_v3$  channels are distinctive in their slow rate of closing upon repolarization (Armstrong and Matteson, 1985; Perez-Reyes, 2003). The voltage-dependent kinetics of  $\text{Ca}^{2+}$  channel closing in human AZF cells was determined after an activating voltage step by measuring the rate of tail current decay at repolarization potentials ranging from  $-40$  to  $-130$  mV. Decaying currents (Fig. 2 C) could be fit with a single exponential time constant ( $\tau_d$ ) that decreased monotonically with repolarization voltage.  $\tau_d$  ranged from  $6.55 \pm 0.60$  ms at  $-40$  mV to  $0.48 \pm 0.06$  ms ( $n = 6$ ) at  $-130$  mV. The function relating  $\tau_d$  to repolarization potential could be fit with a single exponential that included an  $e$ -fold change in  $\tau_d$  per  $36.4$  mV (Fig. 2 C).

**$\text{Ca}^{2+}$  channel pharmacology.** Among the three  $\text{Ca}_v3$  channel subtypes,  $\text{Ca}_v3.1$  is distinctive in its relatively slow kinetics of voltage-dependent activation and inactivation (Klößner et al., 1999). The rapid activation and inactivation kinetics of the  $\text{Ca}_v$  current in human AZF cells suggest that it is either  $\text{Ca}_v3.2$  or  $\text{Ca}_v3.3$ . In this regard,  $\text{Ca}_v3.2$  channels are unique in their extreme sensitivity to block by  $\text{Ni}^{2+}$ .  $\text{Ni}^{2+}$  inhibits  $\text{Ca}_v3.2$  channels with reported  $\text{IC}_{50}$

values between  $2$  and  $13$   $\mu\text{M}$ , whereas  $\text{Ca}_v3.1$  and  $\text{Ca}_v3.3$  channels are  $15$ - to  $20$ -fold less sensitive (Lee et al., 1999; Perez-Reyes, 2003). We found that  $\text{Ni}^{2+}$  reversibly inhibited the T-type  $\text{Ca}^{2+}$  current in human AZF cells with an  $\text{IC}_{50}$  of  $3.0$   $\mu\text{M}$ , identifying it as  $\text{Ca}_v3.2$  (Fig. 3 A).

Trivalent lanthanide elements are among the most potent inorganic inhibitors of T-type  $\text{Ca}^{2+}$  channels (Biagi and Enyeart, 1990; Lansman, 1990; Mlinar and Enyeart, 1993a). Accordingly, gadolinium ( $\text{Gd}^{3+}$ ) was  $\sim 10$ -fold more potent than  $\text{Ni}^{2+}$  as an inhibitor of  $\text{Ca}_v3$  channels in human AZF cells, with an estimated  $\text{IC}_{50}$  of  $245$  nM (Fig. 3 B).

The combined results strongly suggest that  $\text{Ca}_v3.2$  is the predominant  $\text{Ca}^{2+}$  channel expressed by human AZF cells. Although ACTH stimulates cortisol synthesis in bovine AZF cells through mechanisms that require  $\text{Ca}^{2+}$  entry through  $\text{Ca}_v3.2$   $\text{Ca}^{2+}$  channels, this peptide does not directly modulate the activity of T-type  $\text{Ca}^{2+}$  channels in these cells (Mlinar et al., 1993b). At concentrations between  $500$  pM and  $2$  nM, ACTH failed to significantly alter the amplitude of the T-type  $\text{Ca}^{2+}$  current in human AZF cells ( $n = 7$ ; Fig. 3 C).

#### K<sup>+</sup> currents: $I_A$ current

In whole cell patch clamp recordings, a voltage-gated, rapidly inactivating  $\text{K}^+$  current was expressed by each of  $64$  human AZF cells examined. This robust  $I_A$ -type current was activated at potentials positive to  $-50$  mV and averaged  $2,397 \pm 153$  pA in amplitude at a test potential of  $20$  mV, with a mean current density of  $95.0 \pm 7.2$  pA/pF (Fig. 4 A). Experiments were performed to characterize the voltage-dependent gating and kinetic properties of these channels.

**$I_A$ : Voltage-dependent gating.** The voltage dependence of  $I_A$  activation was measured by dividing the peak current amplitudes taken from the steady-state I-V relationship by corresponding amplitudes from the instantaneous I-V (II-V) relationship, as previously described (Mlinar and Enyeart, 1993b). The II-V or open channel I-V provides a measure of membrane conductance at different potentials after all available channels have been activated by a short, strong depolarization. The II-V for  $I_A$  was obtained by activating channels with brief ( $3$  ms) depolarizing steps to  $50$  mV, after which the membrane potential was stepped to new levels between  $40$  and  $-70$  mV.  $\text{K}^+$  current was then measured after  $1$  ms, before a significant change in the number of open channels occurred (Fig. 4 B).

The values obtained upon dividing peak current amplitudes from the steady-state I-V by corresponding amplitudes from the II-V were plotted as the fraction of open channels against membrane potential and fit by a Boltzmann function of the form  $\text{Fraction open} = 1 / [1 + \exp((v_{1/2} - v) / k)]$ , where  $v_{1/2}$  is the voltage at which half of the channels are in the open conformation and  $k$  is the slope factor (Fig. 4 C).

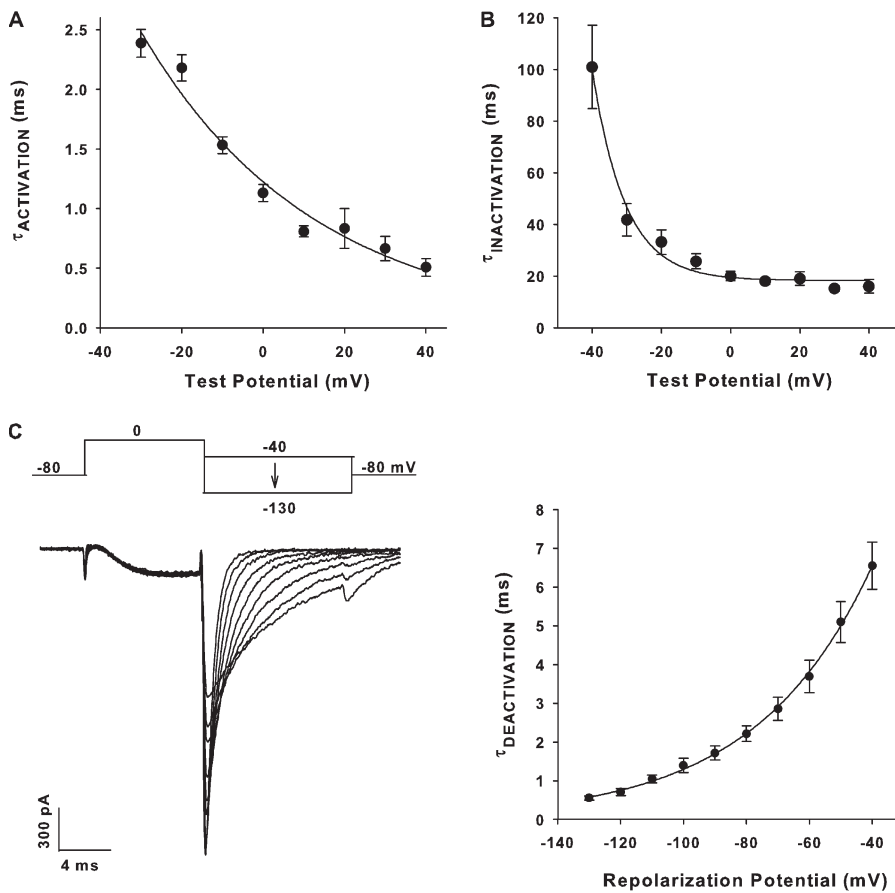


**Figure 2.** Voltage dependence of  $\text{Ca}^{2+}$  current activation, inactivation, and deactivation kinetics. (A) Activation: Currents were activated by 10-ms voltage steps to various test potentials from a holding potential of  $-80$  mV. Current traces were fit with an equation of the form  $I_{Ca} = I_{\infty} [1 - \exp(-T / \tau_a)]^N \exp(-T / \tau_i)$ , where  $\tau_a$  and  $\tau_i$  are the activation and inactivation time constants, and  $N$  is an integer between 1 and 4. Activation time constants (mean  $\pm$  SEM) obtained at various potentials for 21 different cells were plotted as a function of test voltage and fit with a single exponential function. (B) Inactivation:  $\text{Ca}^{2+}$  currents were activated by voltage steps of 300-ms duration at 30-s intervals from a holding potential of  $-80$  mV to test potentials from  $-40$  to  $40$  mV. Inactivation time constants ( $\tau_i$ ) were determined at each test potential by fitting the decaying phase of each current with a single exponential function. Inactivation time constants (mean  $\pm$  SEM) for 11 cells were plotted against voltage and fit with a single exponential. (C) Deactivation kinetics: Decaying tail currents were recorded at potentials ranging from  $-40$  to  $-130$  mV after activation by a 10-ms voltage step to  $0$  mV from a holding potential of  $-80$  mV. Deactivation time constants ( $\tau_d$ ) were determined for each repolarization potential by fitting tail currents with a single exponential function. Deactivation time constants (mean  $\pm$  SEM) from six different cells were plotted against repolarization voltage and fit with an exponential function.

Curves were fit to data points acquired at test potentials between  $-60$  and  $0$  mV. The activation function had a midpoint of  $-37.8$  mV and a  $k$  of  $7.56 \pm 0.62$  mV per  $e$ -fold change in the fraction open (Fig. 4 C).

The voltage-dependent steady-state inactivation of the A-type  $\text{K}^+$  current was studied by applying 10-s conditioning pulses to potentials between  $-90$  and  $-25$  mV in 5-mV increments, followed by activating voltage steps to  $20$  mV. The normalized current was plotted as a function of the conditioning voltage and fitted with the equation  $I / I_{MAX} = 1 / [1 + \exp((v - v_{1/2}) / k)]$ , where  $I_{MAX}$  was the current activated from a holding potential of  $-90$  mV.  $I_A$  inactivation varied as a steep function of voltage with  $v_{1/2}$  equal to  $-51.9 \pm 0.36$  mV ( $n = 5$ ) and a slope factor of  $3.66 \pm 0.31$  mV ( $n = 5$ ) per  $e$ -fold change in the fraction inactivated (Fig. 4 D).

*I<sub>A</sub>: Voltage-dependent activation and inactivation kinetics.* The voltage-dependent activation and inactivation kinetics of the human AZF cell  $I_A$  current were characterized in

whole cell recordings. For activation, current traces from I-V protocols were fit with an equation of the form  $I = I_{\infty} [1 - \exp(-T / \tau_a)]^N [\exp(-T / \tau_i)]$ , where  $\tau_a$  is the activation time constant,  $\tau_i$  is the inactivation time constant, and  $N$  is an integer between 1 and 5. The current traces in Fig. 5 A show  $I_A$  onset kinetics at eight different test potentials. Activation kinetics was clearly sigmoidal, voltage dependent, and accelerated by stronger depolarizations. Onset kinetics was best fit by integer values for  $N$  of 4 or 5.  $\tau_a$  varied from  $2.19 \pm 0.03$  ms to  $0.36 \pm 0.03$  ms ( $n = 5$ ) at test potentials of  $-40$  mV and  $60$  mV, respectively. The function relating  $\tau_a$  and membrane voltage could be expressed as a single exponential with an  $e$ -fold change per 25 mV and a voltage-independent offset of 0.36 ms (Fig. 5 A).

Rapid inactivation kinetics is a defining property of A-type  $\text{K}^+$  currents, including Kv1.4. Inactivation of the  $I_A$  current in human AZF cells could be fit with a single exponential time constant ( $\tau_i$ ) that was voltage independent over a wide range of potentials. Fig. 5 B shows

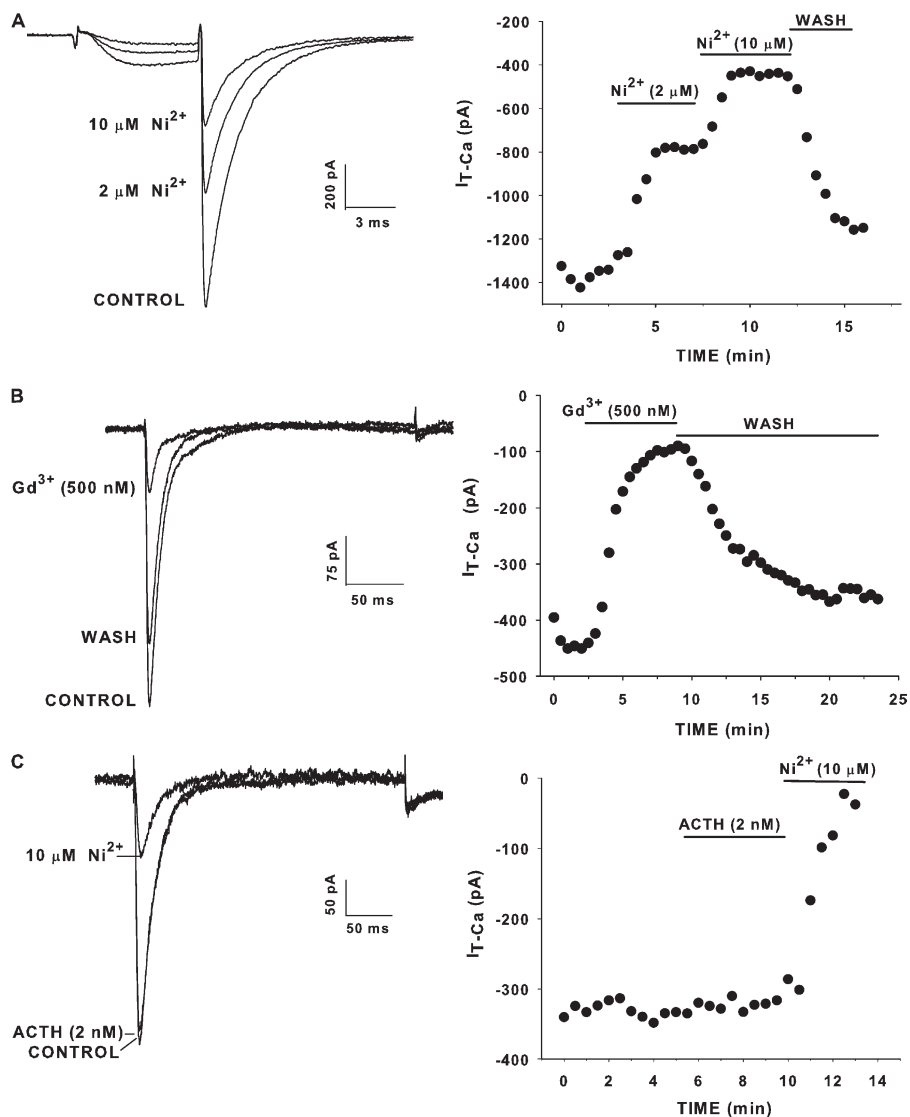


**Figure 3.** Pharmacology of human AZF  $\text{Ca}^{2+}$  current. The effect of  $\text{Ni}^{2+}$ ,  $\text{Gd}^{3+}$ , and ACTH on T-type  $\text{Ca}^{2+}$  current in human AZF cells was measured in whole cell recordings.  $\text{Ca}^{2+}$  currents were activated by short (10 ms) or long (300 ms) depolarizing steps applied at 30-s intervals to 0 mV from a holding potential of  $-80$  mV. Currents were initially recorded in saline and then either  $\text{Ni}^{2+}$ ,  $\text{Gd}^{3+}$ , or ACTH, as indicated. (A)  $\text{Ni}^{2+}$ :  $\text{Ca}^{2+}$  current traces and plot of tail current amplitudes against time for cell superfused with 2 and  $10 \mu\text{M Ni}^{2+}$ . (B)  $\text{Gd}^{3+}$ :  $\text{Ca}^{2+}$  current traces and plot of current amplitudes against time for cell superfused with  $500 \text{ nM Gd}^{3+}$ . (C) ACTH and  $\text{Ni}^{2+}$ :  $\text{Ca}^{2+}$  current traces and plot of current amplitudes for cell superfused with  $2 \text{ nM ACTH}$  and  $10 \mu\text{M Ni}^{2+}$ .

that the decaying component of scaled current traces recorded from a single cell at test potentials between  $-20$  and  $40$  mV was almost super-imposable, with nearly identical  $\tau_i$  values of  $34$  ms. In Fig. 5 C, averaged time constants  $\tau_i$  determined from 15 separate cells are plotted against test voltages. Least squares linear regression analysis of these data yielded a line with a slope not significantly different from zero and an intercept of  $34.2 \pm 0.72$  ms.

#### Noninactivating $\text{K}^+$ current

In addition to the prominent A-type  $\text{K}^+$  current that could be recorded in virtually every healthy human AZF cell, approximately half of these cells also expressed a significant (i.e.,  $>50$  pA) noninactivating  $\text{K}^+$  current that displayed properties of the K2P leak current TREK-1. Specifically, upon voltage clamping the cell at a holding potential of  $-80$  mV and applying voltage steps to  $20$  mV at regular intervals, the noninactivating current typically grew to a stable maximum amplitude over a period of

$10$ – $20$  min (Fig. 6 A). The noninactivating current could be measured at the end of a  $300$ -ms test pulse when  $I_A$  had completely inactivated. Alternatively, the noninactivating current could be observed in isolation by inactivating  $I_A$  with a  $10$ -s depolarizing prepulse (Fig. 6 A, right traces). By itself, the leak-type current appeared to be largely instantaneous with little time- or voltage-dependent activation. This current was present at its highest density on the first day in culture and declined over a period of several days. Overall, this  $\text{K}^+$  current reached a maximum density of  $16.6 \pm 3.1$  pA/pF ( $n = 31$ ) under our recording conditions.

Although the current in human AZF cells resembled TREK-1 expressed in other cells, including bovine AZF and AZG cells, it was important to distinguish it from other members of the K2P family, especially TASK channels, which appear to be the predominant background channel expressed in mouse and rat adrenal cortical cells (Czirják et al., 2000; Czirják and Enyedi, 2002; Enyeart et al., 2002; Enyeart et al., 2004). In this regard, of the

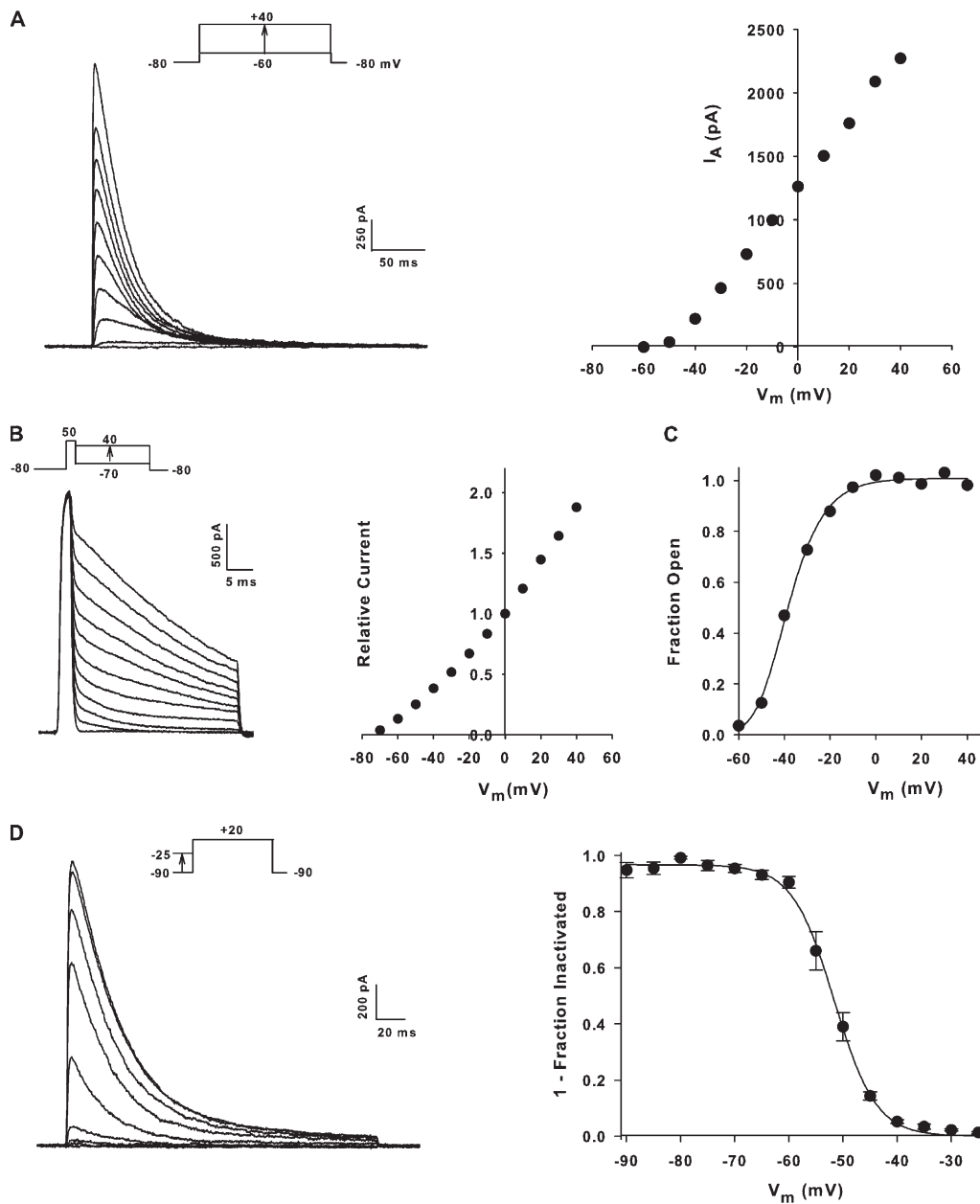


**Figure 4.** Voltage-dependent gating of A-type  $K^+$  current in human AZF cells. (A) I-V relationship: Whole cell  $K^+$  currents were activated by voltage steps to various test potentials applied at 30-s intervals from a holding potential of  $-80$  mV. Peak current amplitudes are plotted against test potential from corresponding current traces shown at left. (B) Open channel I-V relationship: After activating  $I_A$  with a 3-ms voltage step to  $50$  mV from a holding potential of  $-80$  mV, membrane potential was stepped to various values between  $40$  and  $-70$  mV where decaying currents were recorded. (C) Activation: The voltage dependence of  $I_A$  channel activation was determined by dividing peak current amplitudes derived from the steady-state I-V by corresponding values from the II-V. These values were plotted as the fraction of open channels against voltage and fit by a Boltzmann function of the form  $Fraction\ open = 1 / [1 + \exp(v_{1/2} - v) / k]$ , where  $v_{1/2}$  is the voltage at which one half of the channels are in the open conformation and  $k$  is the slope factor. Curve was fit to data points at test potentials between  $-60$  and  $0$  mV. (D) Inactivation: The voltage dependence of steady-state inactivation was measured by applying 10-s prepulses to potentials between  $-90$  and  $-25$  mV, followed by activating voltage steps to  $20$  mV. Normalized current (mean  $\pm$  SEM) for six cells was plotted against conditioning voltage and fitted with the equation  $I / I_{MAX} = 1 / [1 + \exp(v - v_{1/2}) / k]$ , where  $I_{MAX}$  is the current activated from a holding potential of  $-90$  mV and  $v_{1/2}$  is the potential at which half of the channels are inactivated.

15 members of the K2P  $K^+$  channels family, only TREK-1 and TREK-2 are inhibited by cAMP (Enyedi and Czirjak, 2010). We used the diterpene adenylate cyclase activator forskolin to determine whether the noninactivating  $K^+$  current in human AZF cells was TREK-1.

Forskolin effectively inhibited the leak-type  $K^+$  current in human AZF cells, whereas the rapidly inactivating A-type current was unaffected (Fig. 6 A). In seven cells,  $5 \mu M$  forskolin inhibited the noninactivating  $K^+$  current by  $84.2 \pm 4.2\%$  when measured at test potentials

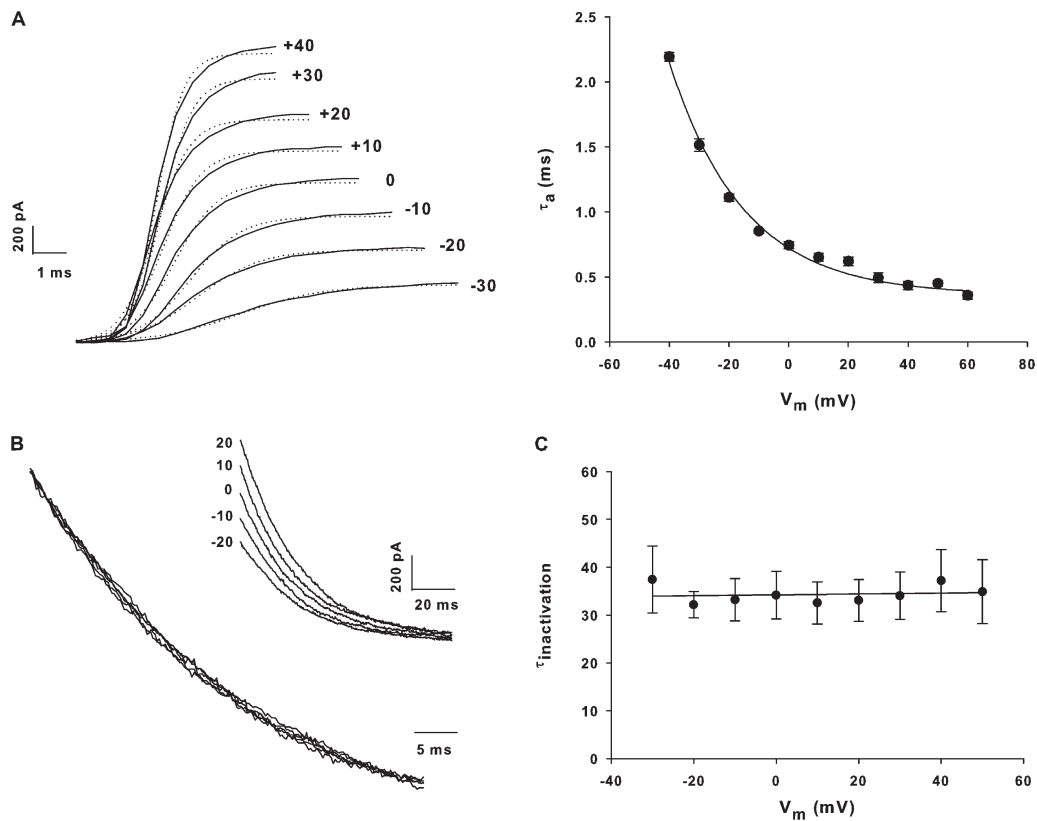


**Figure 5.** Voltage-dependent activation and inactivation kinetics of  $I_A$ . (A) Activation kinetics: Ascending portions of current traces from I-V protocols were fit with an equation of the form  $I = I_{\infty} [1 - \exp(-T / \tau_a)]^N [\exp(-T / \tau_i)]$ , where  $\tau_a$  is the activation time constant,  $\tau_i$  is the inactivation time constant, and  $N$  is an integer between 1 and 5. Current traces at left show onset kinetics at test potentials from -30 to 40 mV.  $\tau_a$  values for five different cells are plotted as mean  $\pm$  SEM at right. Points relating  $\tau_a$  and membrane voltage were fit with a single exponential. (B) Inactivation kinetics:  $I_A$  currents were activated by voltage steps of varying size from a holding potential of -80 mV. Inactivation time constants ( $\tau_i$ ) were determined at each test potential by fitting the decaying phase of the current with a single exponential. Scaled and unscaled (inset) traces recorded at five test potentials are shown. (C)  $\tau_i$  values averaged from 15 different cells are plotted against test voltage as mean  $\pm$  SEM. Data were analyzed with least squares linear regression analysis to yield line with slope of zero and intercept of  $34.2 \pm 0.7$  pA/pF.

of 20 mV. In other experiments, I-V relationships were obtained and showed that the noninactivating  $K^+$  current was outwardly rectifying and blocked by forskolin, although less effectively at test potentials positive to 20 mV (Fig. 6 B). Previously, it had been shown that TREK-1 inhibition by cAMP was voltage dependent and less effective at positive potentials (Bockenbauer et al., 2001). Collectively, these results strongly suggest that the noninactivating current expressed by human AZF cells is TREK-1.

**Activation of the noninactivating current by AA and CDC.** The noninactivating  $K^+$  current was not detectable in approximately one third of freshly plated human AZF cells. This current also spontaneously decreased when human AZF cells were maintained in culture over a period of several days, as previously reported for bTREK-1 channels in bovine AZF cells (Enyeart et al., 2003, 2010). In this regard, of the 15 K2P channels, TREK and TRAAK are distinctive in their activation by AA (Enyedi and Czirjak, 2010). We found that AA markedly increased

the noninactivating  $K^+$  current in human AZF cells even when this current was undetectable under control conditions. In the experiment illustrated in Fig. 7 A, the cell was in culture for 48 h before recording  $K^+$  currents. Only a large A-type  $K^+$  current was detectable during the first 15 min of recording. However, superfusing the cell with 20  $\mu$ M AA rapidly inhibited the A-type current and triggered a slower increase in the noninactivating  $K^+$  current, which reached 2 nA after a 15-min exposure to AA. Overall, 20  $\mu$ M AA increased the noninactivating  $K^+$  current density in human AZF cells from near zero to  $125.6 \pm 44.2$  pA/pF ( $n = 5$ ).

The caffeic acid derivative CDC has also been shown to activate native TREK-1 channels in bovine adrenocortical cells (Danthi et al., 2004). We found that 10–20  $\mu$ M CDC markedly enhanced the activity of the noninactivating  $K^+$  current in human AZF cells, while also suppressing the voltage-gated A-type current. In the experiment illustrated in Fig. 7 B, when CDC was applied to a cell, it increased the current amplitude from an undetectable level to  $>3,000$  pA within 5 min. Overall, 10 or 20  $\mu$ M

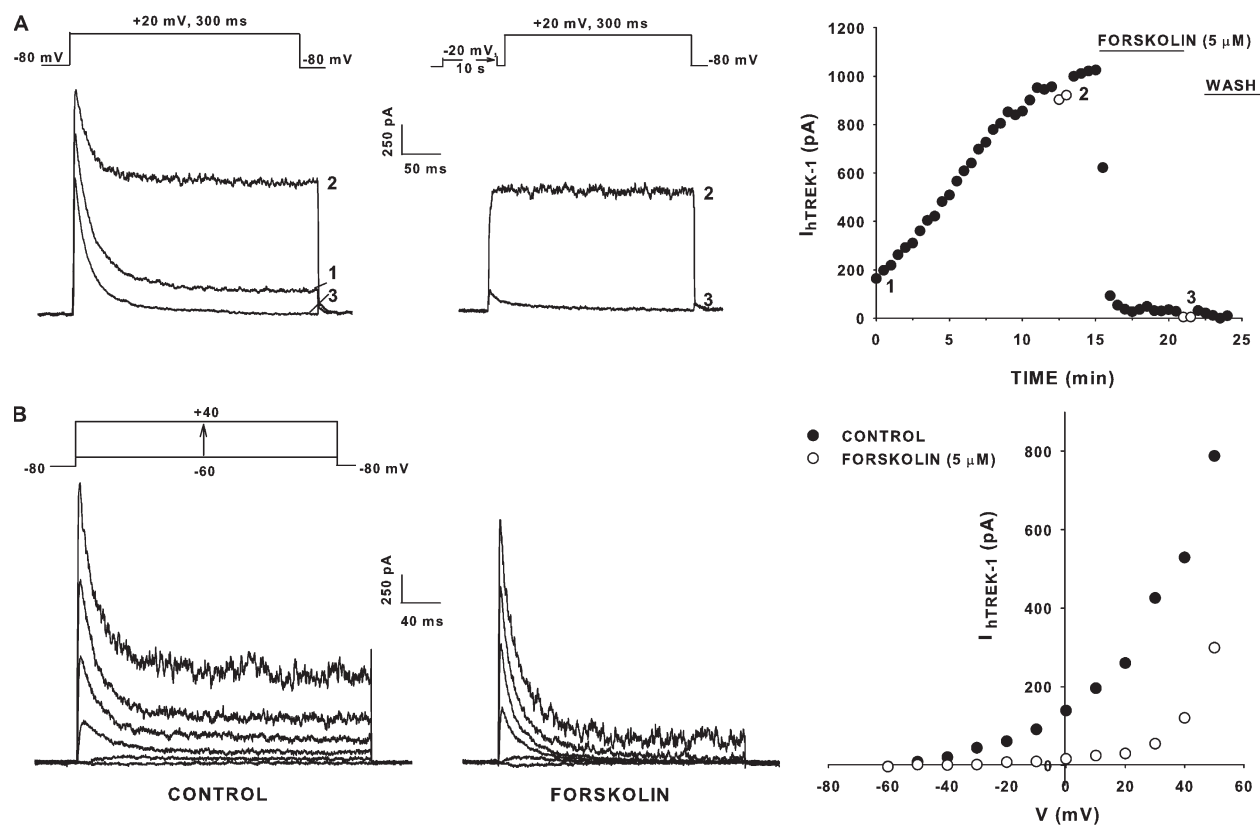


**Figure 6.** Expression of a noninactivating  $K^+$  current inhibited by forskolin in human AZF cells. In whole cell recordings, human AZF cells expressed a noninactivating  $K^+$  current that was inhibited by forskolin. (A) Growth of noninactivating current and selective inhibition by forskolin.  $K^+$  currents were activated by voltage steps to 20 mV applied at 30-s intervals from a holding potential of  $-80$  mV with (right traces) or without (left traces) 10-s prepulses to  $-20$  mV. When the noninactivating current reached a stable maximum, the cell was superfused with  $5 \mu\text{M}$  forskolin. Current amplitudes recorded with (open circles) or without (closed circles) depolarizing prepulses are plotted against time at right. Numbers on the graph correspond to those on the traces at left. (B) Voltage dependence and block by forskolin. The noninactivating  $K^+$  current was allowed to grow to a stable maximum before applying voltage steps at 30-s intervals from a holding potential of  $-80$  mV to test potentials between  $-60$  and  $40$  mV. I-V relationships were obtained before (left traces) and after (right traces) superfusing cells with forskolin. Current amplitudes are plotted against voltage in the absence (closed circles) and the presence (open circles) of forskolin, as indicated.

CDC increased the noninactivating current density from nearly zero to  $40.9 \pm 9.7$  pA/pF ( $n = 7$ ).

The results of experiments with AA and CDC suggested that these agents activated TREK-1 channels, which remained present in the cells but had become inactive after several days in culture. If so, then the K2P current activated by either of these agents could be inhibited by forskolin only if it were TREK. The experiment illustrated in Fig. 7 C shows that forskolin effectively inhibited the current activated by  $10 \mu\text{M}$  CDC. Similar results were obtained in three experiments.

**TREK-1 and membrane potential.** The activation of the noninactivating  $K^+$  current by AA and its inhibition by forskolin were tightly coupled to the membrane potential measured under current clamp. In the experiment illustrated in Fig. 7 D, the inhibition of the putative TREK-1 current by forskolin depolarized the cell by 34 mV, whereas subsequent activation of this current by AA produced a 42-mV hyperpolarization. In a total of five AZF

cells, the activation of the noninactivating  $K^+$  current by AA increased the membrane potential by  $-37.0 \pm 4.2$  mV ( $n = 5$ ). In contrast, inhibition of this current by forskolin depolarized AZF cells by  $30.3 \pm 4.2$  mV ( $n = 3$ ).

**Inhibition of the noninactivating current by ACTH.** ACTH stimulates cortisol secretion by activation of a  $G_s$ -coupled MC2R melanocortin receptor, leading to the activation of adenylate cyclase (Mountjoy et al., 1992). If the noninactivating  $K^+$  current in human AZF cells is caused by TREK channels, then it should be inhibited by ACTH. The putative TREK-1 current expressed by human AZF cells was potently and effectively inhibited by ACTH (Fig. 8 A). At concentrations of 500 pM and 1 nM, ACTH inhibited the noninactivating current by  $90.2 \pm 4.9\%$  ( $n = 6$ ) and  $86.0 \pm 4.8\%$  ( $n = 5$ ), respectively. In other experiments, ACTH produced near complete inhibition of the noninactivating current at concentrations as low as 20 pM. Inhibition of this current by ACTH was voltage independent over a wide range of test potentials.

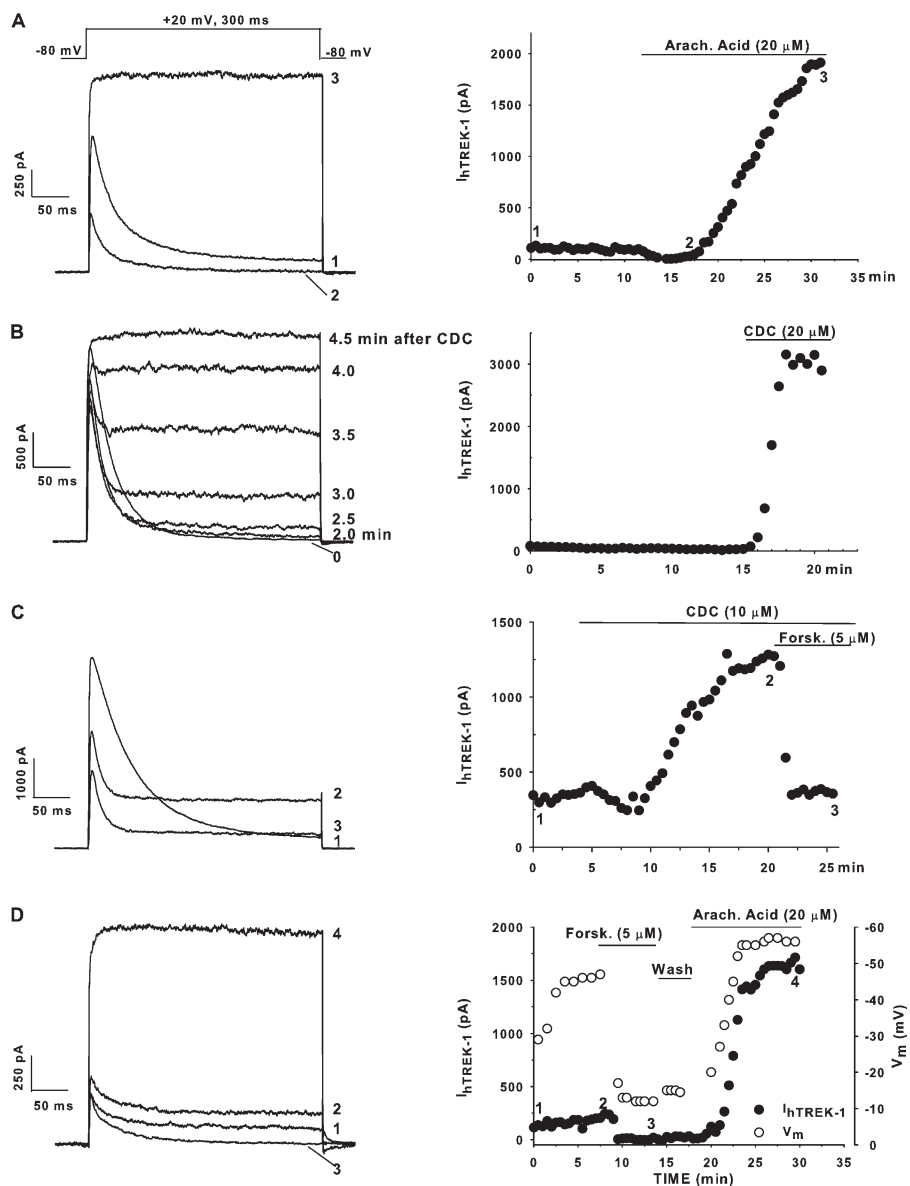


**Figure 7.** AA and CDC activate the noninactivating K<sup>+</sup> current in human AZF cells. Whole cell recordings of K<sup>+</sup> currents were made from human AZF cells that had been in culture for 48–72 h. After recording K<sup>+</sup> currents in standard saline, cells were superfused with AA or CDC. (A) Effect of AA. K<sup>+</sup> currents were activated by voltage steps to 20 mV applied at 30-s intervals from a holding potential of –80 mV. After 15 min, the cell was superfused with 20 μM AA. Numbers on current traces correspond to those in the plot of current amplitudes against time at right. (B) Effect of CDC. K<sup>+</sup> currents were activated as described in A. After 15 min, the cell was superfused with 20 μM CDC. Traces show currents at times indicated after the superfusion of CDC. Noninactivating current amplitudes are plotted against time in the graph at right. (C) Forskolin inhibits CDC-activated current. K<sup>+</sup> currents were activated as described in A. Currents were initially recorded in saline, then in 10 μM CDC, followed by CDC and 5 μM forskolin, as shown. Numbers on traces correspond to those on the plot of noninactivating current amplitudes at right. (D) K<sup>+</sup> current expression and membrane potential. K<sup>+</sup> currents and membrane potential were measured at 30-s intervals by switching between voltage clamp and current clamp. The cell was superfused with 5 μM forskolin and 20 μM AA at the indicated times. Numbers on traces in the left panel correspond to those in the plot of current amplitudes at right.

In the experiment illustrated in Fig. 8 B, 1 nM ACTH selectively and completely inhibited the noninactivating K<sup>+</sup> current at potentials from –50 to 40 mV.

**Inhibition of the noninactivating K<sup>+</sup> current by AngII.** Although ACTH is the principal peptide hormone regulating cortisol secretion, AngII may also stimulate secretion in some species, including humans (Lebrethon et al., 1994). AngII inhibits multiple K<sup>+</sup> channels, including TREK-1, through activation of a G<sub>i</sub>-coupled AT<sub>1</sub> receptor (Enyeart et al., 2005; Enyedí and Czirják, 2010). Accordingly, we found that AngII also inhibited the noninactivating K<sup>+</sup> current in human AZF cells, although it was less effective than ACTH. In the experiment shown in Fig. 9, 10 nM AngII selectively inhibited the noninactivating K<sup>+</sup> current by 57%, without altering the rapidly inactivating A-type current. Subsequent superfusion of

the cell with 1 nM ACTH resulted in near complete inhibition of the remaining noninactivating current. Overall, in nine cells, 5 or 10 nM AngII inhibited the noninactivating K<sup>+</sup> current by  $72.4 \pm 6.6\%$ , without any measurable effect on the A-type K<sup>+</sup> current. These results indicate that a large fraction of the ACTH-sensitive K<sup>+</sup> current expressed by human AZF cells is also inhibited by AngII and further suggest that this current is TREK-1.

**Northern blot analysis of human AZF ion channel mRNAs.** Whole cell patch clamp experiments indicated that human AZF cells express at least three specific ion channels that we tentatively identified as Ca<sub>v</sub>3.2, Kv1.4, and TREK-1. Northern blot analysis showed that mRNA transcripts coding for each of these channels were robustly expressed by human adrenocortical cells (Fig. 10).

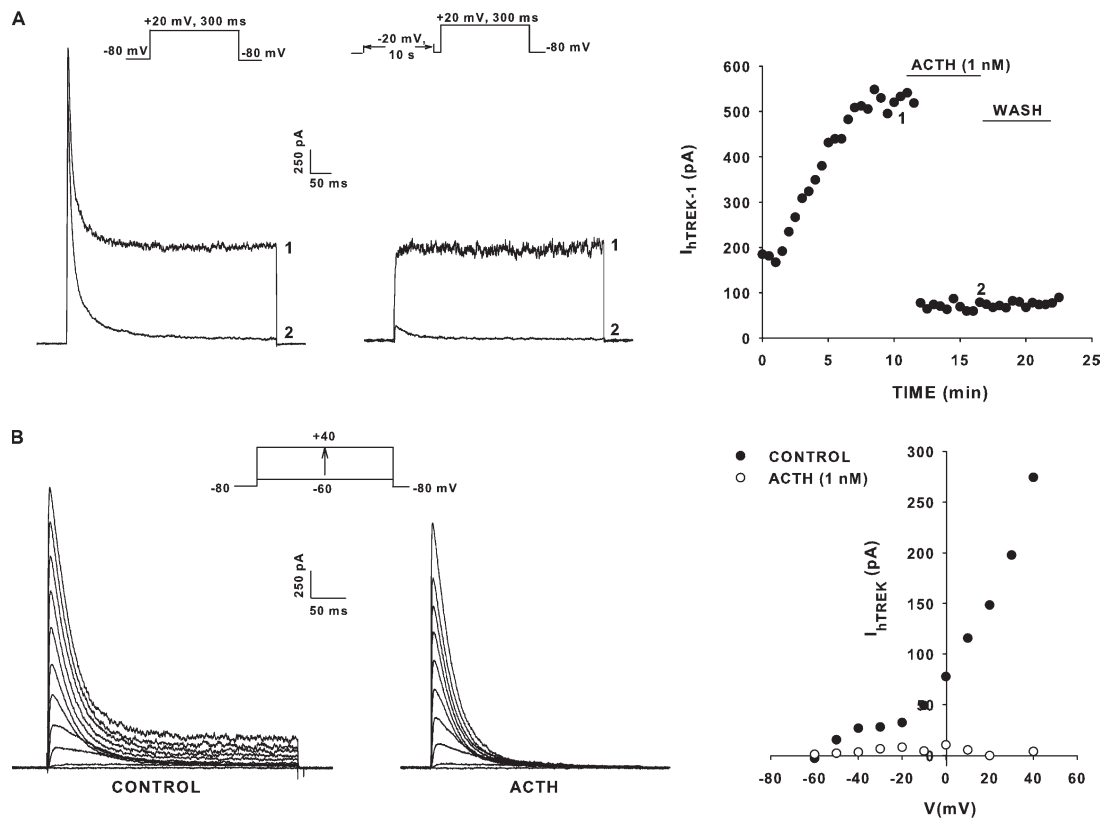


**Figure 8.** ACTH inhibits the noninactivating  $K^+$  current in human AZF cells. (A) ACTH selectively inhibits noninactivating current.  $K^+$  currents were activated by voltage steps to 20 mV applied at 30-s intervals from a holding potential of  $-80$  mV with (right traces) or without (left traces) 10-s prepulses to  $-20$  mV. When the noninactivating current reached a stable maximum, the cell was superfused with 1 nM ACTH. Current amplitudes are plotted against time at right. (B) Voltage-independent inhibition by ACTH. After the noninactivating  $K^+$  current reach a maximum,  $K^+$  currents were activated by voltage steps applied at 30-s intervals from a holding potential of  $-80$  mV to test potentials between  $-60$  and 40 mV. I-V relationships were recorded before (left traces) and after (right traces) superfusing the cell with 1 nM ACTH. Noninactivating current amplitudes are plotted against voltage in the absence (closed circles) and presence (open circles) of ACTH in the graph at right.

*Effect of ACTH, AngII, and CDC on cortisol secretion.* The inhibition of the noninactivating current in human AZF cells by ACTH and AngII suggests that both of these peptides could stimulate cortisol secretion by human AZF cells through a mechanism requiring depolarization-dependent  $Ca^{2+}$  entry. We compared the effect of ACTH and AngII on cortisol secretion by human AZF cells in culture at times ranging from 2 to 24 h. We found that

AngII, as well as ACTH, stimulated cortisol secretion from human AZF cells. However, in contrast to ACTH, which produced both rapid and delayed increases, AngII significantly increased the quantity of cortisol produced only after delays exceeding 2 h (Fig. 11, A and B). Overall, the effectiveness of the two peptides in stimulating cortisol secretion paralleled their effectiveness as inhibitors of the noninactivating  $K^+$  current in these cells. In

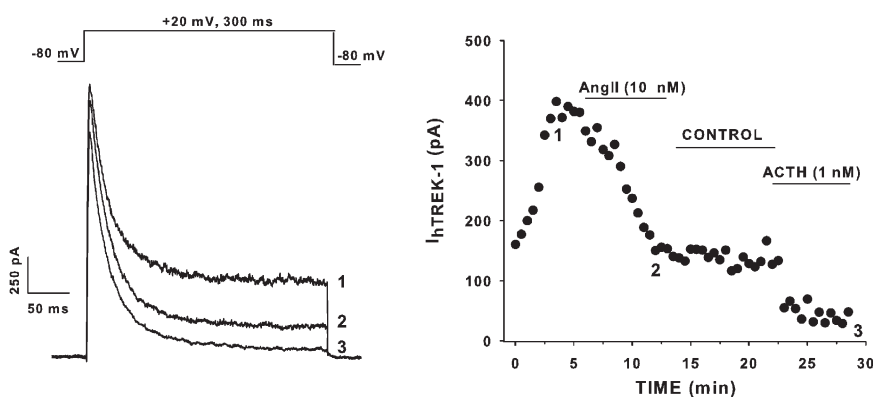


**Figure 9.** AngII selectively inhibits the noninactivating  $K^+$  current in human AZF cells.  $K^+$  currents were activated by voltage steps to 20 mV applied at 30-s intervals from a holding potential of  $-80$  mV. When the noninactivating current reached a maximum (trace #1), the cell was superfused with 10 nM AngII. After AngII block stabilized (trace #2), control saline was superfused, followed by 1 nM ACTH (trace #3), as indicated. Current amplitudes are plotted against time in the graph at right. Numbers next to the traces (left) correspond to those on the plot of noninactivating current amplitudes in the graph at right.

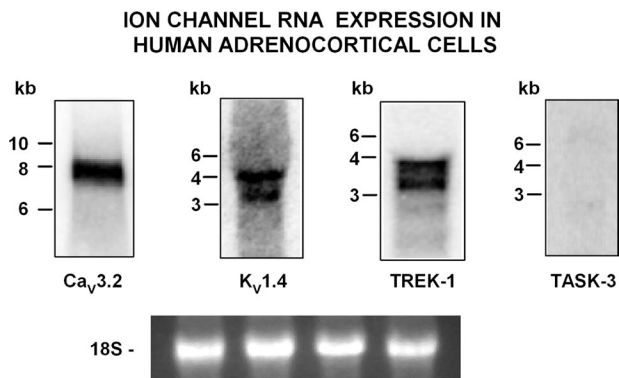


**Figure 10.** Ion channel gene expression in the human adrenal cortex. Northern autoradiogram with total RNA isolated from human adrenocortical cells isolated and cultured for 24 h as described in Materials and methods. Northern blot membrane was separated into four equal lanes each containing 10  $\mu$ g of total RNA for hybridization with specific channel probe, as described in Materials and methods. Northern autoradiograms were imaged after 4-h exposure to imaging screen for each probe. 18S lanes are shown as evidence of even loading. Bands correspond to transcripts of one distinct band of  $\sim$ 7.8–8 kb for  $Ca_v3.2$ ; two bands of  $\sim$ 4.4 and 3.4 kb for  $K_v1.4$ ; two distinct bands of  $\sim$ 3.6 and 4.0 kb, with a weaker band at 2.8 kb for TREK-1; and for TASK-3, no discernible bands were seen after 4-h exposure.

three separate experiments, after 24 h, ACTH and AngII increased cortisol production by  $493 \pm 41\%$  and  $307 \pm 26\%$ , respectively ( $n = 3$ ). The combined effects of ACTH and AngII on cortisol secretion were additive, as might be expected for peptides that activate different G-protein-coupled signaling pathways (Fig. 11 B).

In a previous study on bovine AZF cells, we showed that, at concentrations  $>10 \mu$ M, CDC could both overcome the inhibition of bTREK-1 by ACTH and inhibit ACTH-stimulated cortisol secretion (Danthi et al., 2004). In the present study, we found that 15  $\mu$ M CDC completely inhibited both ACTH- and AngII-stimulated cortisol secretion, measured at 6 and 24 h. In contrast, CDC was far less effective at inhibiting unstimulated secretion (Fig. 11 B).

If ACTH- and AngII-stimulated cortisol secretion by AZF cells is coupled to depolarization through the activation of  $Ca_v3.2$  channels, then selective antagonists should inhibit this T-type current and secretion with similar potency. Mibefradil is an organic  $Ca^{2+}$  antagonist that preferentially blocks T-type  $Ca^{2+}$  channels (Mishra and Hermsmeyer, 1994). At a concentration of 2.5  $\mu$ M, mibefradil inhibited the  $Ca_v3.2$  current in human AZF cells by  $74.5 \pm 6.1\%$  ( $n = 3$ ; Fig. 12 A, left and right). Accordingly, at this same concentration, mibefradil effectively inhibited both ACTH- and AngII-stimulated cortisol secretion measured at 2 and 24 h (Fig. 12 B, left and right). In contrast, mibefradil had no effect on unstimulated secretion. In the experiment illustrated in Fig. 12 B, mibefradil reduced ACTH-stimulated secretion at 2 h and 24 h by  $53.3 \pm 4.6\%$  and  $42.7 \pm 9.2\%$ ,

respectively. In the same experiment, AngII-stimulated secretion was reduced at 2 h and 24 h by  $37.1 \pm 2.7\%$  and  $46.0 \pm 3.4\%$ , respectively.

## DISCUSSION

In this study, we discovered that normal human AZF cells express voltage-gated, rapidly inactivating  $Ca^{2+}$  and  $K^+$  currents and a noninactivating leak-type  $K^+$  current. Characterization of these currents in whole cell patch clamp recordings with respect to voltage-dependent gating and pharmacology, in conjunction with Northern blot analysis, identified these channels as  $Ca_v3.2$ ,  $K_v1.4$ , and TREK-1. Of these three channels, the noninactivating  $K^+$  channel was potently and selectively inhibited by ACTH at concentrations that stimulate cortisol secretion. AngII also inhibited the noninactivating  $K^+$  current and stimulated delayed increases in cortisol secretion from human AZF cells. The activation and inhibition of TREK-1 in human AZF cells were shown to be coupled to membrane hyperpolarization and depolarization, respectively. Mibefradil inhibited  $Ca_v3.2$   $Ca^{2+}$  currents as well as ACTH- and AngII-stimulated cortisol secretion at identical concentrations. In addition to identifying the major ion channels expressed by human AZF cells and providing the first description of the modulation of one of these channels by the peptide hormones that physiologically regulate cortisol secretion, these results suggest a specific mechanism wherein ACTH and AngII receptor activation is coupled to depolarization-dependent  $Ca^{2+}$  entry and secretion by the inhibition of TREK-1 channels.

### Comparison of human, bovine, and rodent AZF cell ion currents

Bovine, rat, and mouse AZF cells have been used as models for human cortisol secretion (Simpson and Waterman, 1988; Waterman, 1994). Because ion channels act pivotally in the physiology of cortisol secretion, the relevance of the model systems to human AZF cell secretion rests on the similarity of their ion channels. The ion channels of normal bovine and rat AZF cells, and a mouse AZF cell line, have been described in patch clamp studies. Although bovine AZF cell ion channels are remarkably similar to those of humans, channels expressed in rodent AZF cells are quite different. Specifically, rat AZF cells express only voltage-gated T- and L-type  $Ca^{2+}$  channels and a slowly inactivating A-type  $K^+$  current, whereas no leak-type current similar to TREK-1 is detectable (Barbara and Takeda, 1995). Mouse Y1 adrenocortical cells express only a  $Ca^{2+}$ -dependent  $K^+$  current and two types of voltage-gated  $Ca^{2+}$  currents (Tabares et al., 1985).

In contrast to rat and mouse, bovine AZF cells appear to express the same three ion channels as normal human cells. Importantly, TREK-1 is the primary or sole  $K_2P$  channel present in both bovine and human AZF cells. In both cells, TREK-1 channels are potently inhibited

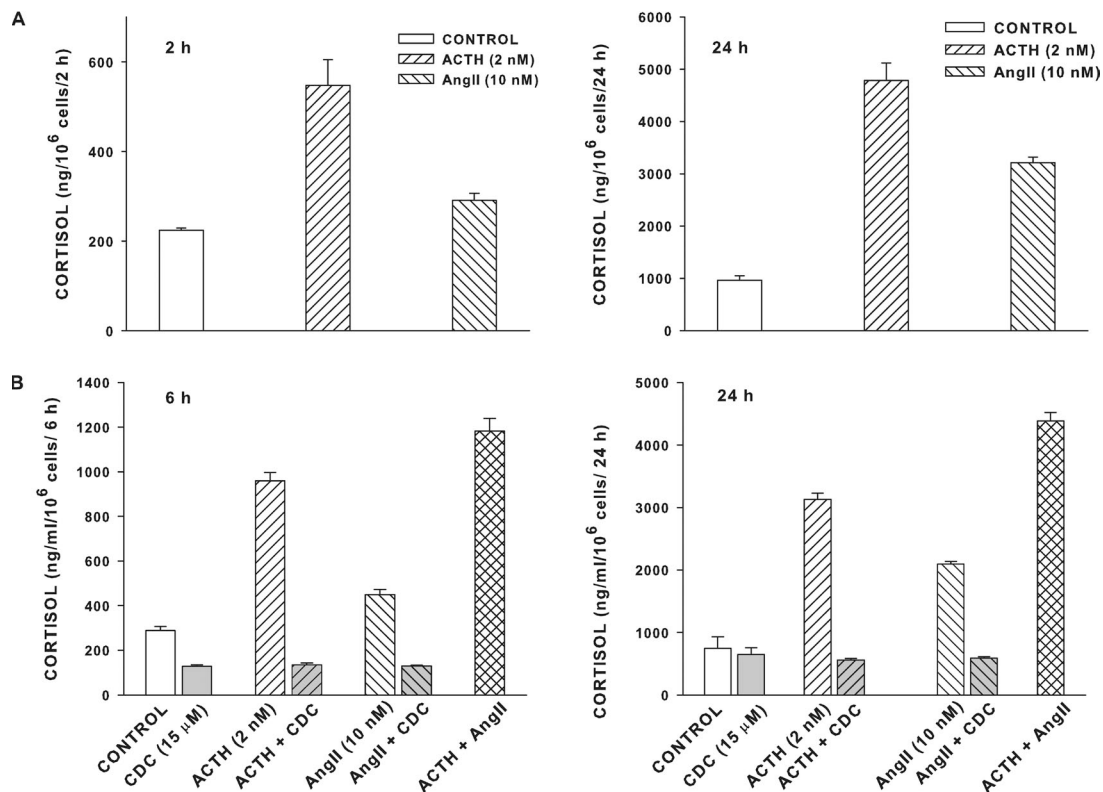


**Figure 11.** Effect of ACTH, AngII, and CDC on cortisol secretion from human adrenal fasciculata cells. Human AZF cells were plated as described in Materials and methods. After 48 h, defined medium was aspirated and replaced with the same medium either without (control) or with ACTH, AngII, or CDC, as shown. Media was collected at the indicated times, and cortisol concentration was determined by EIA as described in Materials and methods. Cortisol values expressed are the mean  $\pm$  SEM of duplicate determinations from triplicate plates. (A) Cortisol was measured from media samples collected 2 (left) and 24 h (right) after either no treatment (control) or treatment with 2 nM ACTH or 10 nM AngII, as indicated. (B) Cortisol was measured from media samples collected after 6 (left) or 24 h (right) after either no treatment (control) or treatment with 15  $\mu$ M CDC, 2 nM ACTH, ACTH plus CDC, 10 nM AngII, AngII plus CDC, or ACTH plus AngII, as indicated.

by ACTH and AngII at concentrations that stimulate cortisol secretion (Mlinar et al., 1993a). Thus, it would appear that bovine AZF cells are superior to either mouse or rat as an authentic model for cortisol secretion in humans.

The human H295R adrenocortical cell line has been used as a model for corticosteroid secretion in over 400 published studies. Although the ion channels in these cells have not been systematically studied, they appear to differ fundamentally from those of normal human AZF cells. Specifically, these cells express neuronal  $\omega$ -conotoxin N-type channels that function in AngII-stimulated cortisol secretion (Aritomi et al., 2011). We have also found that H295R cells express other neuron-specific ion channels, but no TREK-1  $K^+$  currents could be detected (unpublished data). Collectively, these results indicate that the electrical properties of H295R cells differ markedly from those of normal human AZF cells. Furthermore, the ion channels expressed by this cell line may vary with time and culture conditions. Therefore, the results of secretion studies obtained using these cells as a model for human cells should be interpreted with caution.

The  $Ca^{2+}$  and  $K^+$  currents that we have identified in human AZF cells differ fundamentally from those described in a previous study on human AZG cells (Payet et al., 1994). Specifically, in the AZG study, a large non-inactivating  $Ca^{2+}$  current that inexplicably reached a maximum amplitude at 70 mV was reported in addition to a slowly activating voltage-gated delayed rectifier  $K^+$  current. No  $K^+$  current resembling TREK-1 was observed.

#### Voltage-gated $Ca^{2+}$ channels in human AZF cells

Whole cell patch clamp recordings showed that human AZF cells express predominantly or exclusively low voltage-activated  $Ca_v3.2$  T-type  $Ca^{2+}$  channels. These channels resembled native and cloned  $Ca_v3.2$  channels with respect to voltage-dependent gating and kinetic properties and pharmacology (Chen and Hess, 1990; Mlinar et al., 1993b; Perez-Reyes et al., 1998; Klöckner et al., 1999). In particular, the potent inhibition of the T-type  $Ca^{2+}$  current by  $Ni^{2+}$  ( $IC_{50} = 3.0 \mu M$ ) clearly identified this current as  $Ca_v3.2$  among the three  $Ca_v3$  subtypes. In contrast,  $Ca_v3.1$  and  $Ca_v3.3$  are blocked by  $Ni^{2+}$  with  $IC_{50}$  values  $> 100 \mu M$  (Lee et al., 1999). The T-type  $Ca^{2+}$

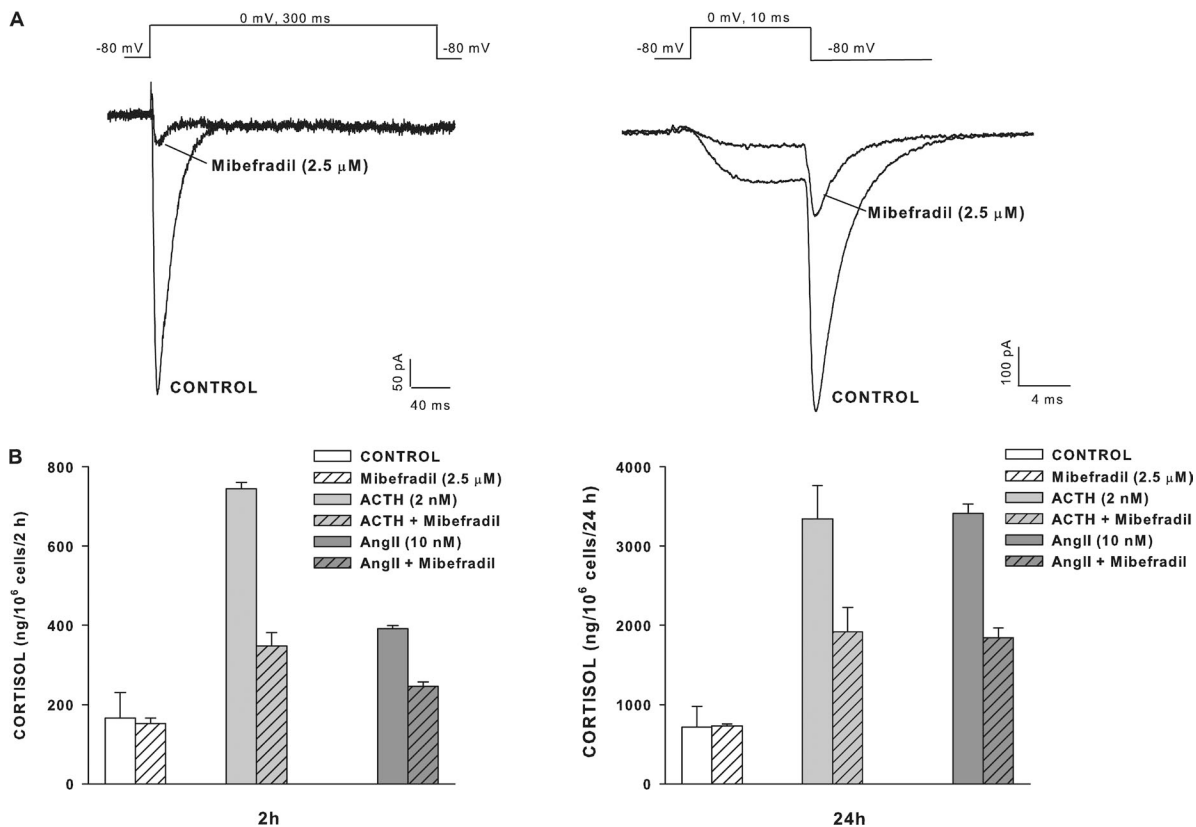


**Figure 12.** Mibefradil inhibits  $\text{Ca}_v3.2 \text{Ca}^{2+}$  currents and cortisol secretion in human AZF cells. The effect of mibefradil on  $\text{Ca}_v3.2$  current and cortisol secretion stimulated by ACTH and AngII was measured in human AZF cells. (A)  $\text{Ca}_v3.2$  currents were activated by long (300 ms; left) or short (10 ms; right) depolarizing steps applied at 30-s intervals to 0 mV from a holding potential of  $-80$  mV. Current traces were recorded in control saline and  $2.5 \mu\text{M}$  mibefradil, as indicated. (B) Human AZF cells were plated as described in Materials and methods. After 48 h, defined medium was aspirated and replaced with the same media with or without mibefradil for 20 min, followed by media containing mibefradil and either 2 nM ACTH or 10 nM AngII, as indicated. Media were collected after 2 (left) or 24 h (right), and cortisol was determined by EIA as described in Materials and methods. Cortisol values expressed are the mean  $\pm$  SEM of duplicate determinations from triplicate plates.

channels of humans and bovine AZF cells are clearly different from those of rats, which are blocked by  $\text{Ni}^{2+}$  with an  $\text{IC}_{50}$  of  $132 \mu\text{M}$  (Durroux et al., 1988).

In human AZF cells,  $\text{Ca}_v3.2$  channels probably provide the major portal for depolarization-dependent  $\text{Ca}^{2+}$  entry. However, it does not appear that ACTH enhances  $\text{Ca}^{2+}$  entry through direct modulation of these channels because this peptide had no effect on the  $\text{Ca}_v3.2$  current. Accordingly, ACTH does not enhance the  $\text{Ca}_v3.2$  current in either bovine or rat AZF cells (Mlinar et al., 1993b; Barbara and Takeda, 1995).

#### Voltage-gated A-type $\text{K}^+$ current in human AZF cells

The voltage-gated, rapidly inactivating A-type current was the largest current present in virtually every human AZF cell examined. This A-type current resembled the  $\text{Kv}1.4$  current in bovine AZF cells with respect to voltage-dependent gating and kinetic properties (Mlinar and Enyeart, 1993b). In particular, activation kinetics was voltage dependent but reached a voltage-independent offset at potentials positive to 0 mV. However, as previously

observed in bovine cells, inactivation kinetics of the human A-type current was independent of voltage over a wide range of test potentials. Furthermore, the human and bovine A-type currents both inactivate rapidly with similar time constants (Mlinar and Enyeart, 1993b). The A-type  $\text{K}^+$  currents of bovine and human AZF cells are inhibited similarly by CDC and AA (Danthi et al., 2003, 2004). Overall, our patch clamp experiments and Northern blot results indicate that the A-type  $\text{K}^+$  current in human AZF cells is  $\text{Kv}1.4$ . In contrast, the A-type  $\text{K}^+$  current in rat AZF cells inactivates 10 to 20 times more slowly than that of human and bovine cells and is therefore not likely  $\text{Kv}1.4$  (Barbara and Takeda, 1995).

The function of these large A-type  $\text{K}^+$  currents in human AZF cells has not been determined. In vertebrates, A-type  $\text{K}^+$  currents are present in excitable cells, ranging from cardiac and smooth muscle cells to peripheral and central neurons where they regulate action potential spacing and duration (Belluzzi et al., 1985; Clark et al., 1988; Cooper and Shrier, 1989; Imaizumi et al., 1990; Ficker and Heinemann, 1992). Although AZF cells are not

typically classified as excitable, the presence of action potential-like waveforms from AZF cells of several species suggests that this form of electrical activity could be present in the intact gland under physiological conditions (Matthews and Saffran, 1968, 1973; Natke and Kabela, 1979; Lymangrover et al., 1982; Quinn et al., 1987; Barbara and Takeda, 1995). In the absence of action potentials, this robust current has no obvious purpose in the human AZF.

#### Background K<sup>+</sup> channels in human AZF cells

The noninactivating K<sup>+</sup> current expressed in human AZF cells displayed several properties which, collectively, identify it as TREK-1. First, in whole-cell recordings where the membrane potential was held at -80 mV, the noninactivating current grew to a stable maximum value over a period of minutes. When human or mouse TREK-1 channels are heterologously expressed in *Xenopus laevis* oocytes, TREK-1 activity can be increased or decreased over a period of minutes by, respectively, hyperpolarizing or depolarizing the cell membrane (Segal-Hayoun et al., 2010; Bagriantsev et al., 2012). The molecular mechanism that underlies the slow voltage-dependent modulation of open probability is currently unknown, but the phenomenon appears to be specific to TREK among the K2P channels.

Similar to TREK-1 currents in other cells including bovine AZF, the human noninactivating current included a large instantaneous component that was outwardly rectifying. Furthermore, the selective and near complete inhibition of the noninactivating K<sup>+</sup> current in human AZF cells by forskolin and ACTH provides additional evidence that the noninactivating current is TREK-1 and that this channel is the predominant K2P channel expressed by these cells. In this regard, the effective inhibition of the noninactivating K<sup>+</sup> current by forskolin provides convincing evidence that this current is either TREK-1 or TREK-2 because these are the only K2P channels inhibited by cAMP-dependent pathways (Enyedi and Czirják, 2010). Because TREK-2 does not appear to be expressed in the adrenal cortex (its EST profile on Unigene is reported as 0/32935 in the human adrenal), it is highly likely that the human AZF channel is TREK-1 (Lesage et al., 2000).

It was also observed that forskolin was less effective at inhibiting the noninactivating K<sup>+</sup> current at potentials positive to 20 mV. Accordingly, it was previously reported that TREK-1 inhibition by cAMP is voltage dependent and less effective at positive potentials (Bockenhauer et al., 2001). In contrast to forskolin, the inhibition of TREK-1 by ACTH was voltage independent. In this regard, ACTH may produce effects in bovine AZF cells through multiple cAMP-dependent and -independent mechanisms (Omura et al., 2007; Liu et al., 2010).

The remarkable increase in the amplitude of the noninactivating K<sup>+</sup> current stimulated by AA and CDC in

human AZF cells provided further evidence that this current is TREK-1 and indicates that these cells express thousands of these channels. Of the K2P family, AA activates only the mechano-gated subgroup comprised of TREK-1, TREK-2, and TRAAK channels, and CDC has only been shown to activate TREK-1 (Danthi et al., 2004; Enyedi and Czirják, 2010). Accordingly, the inhibition of the CDC-activated K<sup>+</sup> current in human cells by forskolin argues that it is TREK-1.

It is not clear why human AZF cells express leak-type channels at this high density when only a small fraction of these might be sufficient to establish a resting potential near the K<sup>+</sup> equilibrium potential. Regardless, experiments with CDC and AA indicated that TREK-1 is the predominant K2P channel expressed in human AZF cells. They further showed that after AZF cells are maintained in culture for several days, their TREK-1 channels can exist in a dormant form that can still be activated by CDC or AA.

#### Inhibition of the noninactivating K<sup>+</sup> current by ACTH and AngII

The inhibition of the noninactivating K<sup>+</sup> current by ACTH and AngII is the first demonstration of the modulation of a specific ion current by either of these two peptide hormones in normal human AZF cells and provides additional proof that this current is TREK-1. TREK channels are the only K2P channels inhibited by the activation of both G<sub>s</sub>- and G<sub>q</sub>-coupled receptors. In bovine AZF cells, ACTH activates a G<sub>s</sub>-coupled MC2R receptor, leading to TREK-1 inhibition through PKA-dependent phosphorylation and perhaps other cAMP-dependent pathways (Mountjoy et al., 1992; Liu et al., 2008). The near complete inhibition of the noninactivating K<sup>+</sup> current further argues that TREK-1 is the predominant leak-type K<sup>+</sup> channel in human AZF cells.

In our experiments, the inhibition of noninactivating K<sup>+</sup> current by ACTH and AngII was measured under identical conditions, with the pipette solutions containing 2 mM MgATP and [Ca<sup>2+</sup>]<sub>i</sub> strongly buffered by 11 mM BAPTA. Therefore, inhibition by either peptide was likely independent of any increases in [Ca<sup>2+</sup>]<sub>i</sub> (Augustine et al., 2003; Fakler and Adelman, 2008). In this regard, in bovine AZF cells, AngII inhibits TREK-1 currents by separate Ca<sup>2+</sup>- and ATP hydrolysis-dependent pathways (J.J. Enyeart et al., 2005, 2011; Liu et al., 2007). It will be interesting to determine whether AngII inhibits the noninactivating K<sup>+</sup> current in human cells by dual signaling pathways.

#### TREK-1 K<sup>+</sup> channels, membrane potential, and cortisol secretion

Experiments that showed a close correlation between the expression of TREK-1 current and membrane potential suggested a model for ACTH- and AngII-stimulated cortisol secretion by human AZF cells that relies on

depolarization-dependent  $\text{Ca}^{2+}$  entry. Accordingly, in secretion experiments, we showed that the selective T-type  $\text{Ca}^{2+}$  channel antagonist mibefradil effectively inhibited  $\text{Ca}_v3.2$  channels and cortisol secretion stimulated by either ACTH or AngII. Furthermore, CDC inhibited cortisol secretion stimulated by these two peptide hormones at the same concentration that markedly increased TREK-1 activity. In previous studies, we found similar effects of these two agents on  $\text{Ca}_v3.2$ , TREK-1, and cortisol secretion in bovine AZF cells (Gomora et al., 2000; Danthi et al., 2004).

Overall, the results of patch clamp and secretion studies suggest a model for cortisol secretion by human AZF cells in which ACTH and AngII receptor activation is coupled to depolarization and the activation of  $\text{Ca}_v3.2$  channels through TREK-1 inhibition. In this regard, the action potential-like waveforms that have been recorded from AZF cells of several species suggest that, under physiological conditions in the intact adrenal gland, these cells are excitable. It is possible that TREK-1 inhibition induces  $\text{Ca}^{2+}$ -dependent action potentials in human AZF cells, driven by opposing  $\text{Kv}1.4$  and slowly deactivating  $\text{Ca}_v3.2$  currents. However, in current clamp recordings from dissociated human AZF cells in culture, we have not detected the presence of action potentials.

If human AZF cells do not generate action potentials, it is not clear how the strong depolarization produced by ACTH and AngII through TREK-1 inhibition leads to sustained  $\text{Ca}^{2+}$  entry via the rapidly inactivating  $\text{Ca}_v3.2$  channels and subsequent prolonged increases in cortisol secretion. It is possible that, at concentrations sufficient to only partially inhibit TREK-1, ACTH and AngII depolarize cells to a potential where a sustained “window” current through  $\text{Ca}_v3.2$  persists.

The function of the large  $\text{Kv}1.4$  current expressed by nearly every human AZF cell remains to be clarified. This  $\text{K}^+$  current, averaging one to several nanoamperes in amplitude, by rapidly repolarizing the AZF cells at a rate of 100 mV/ms or more, could provide for the repolarization phase of a  $\text{Ca}^{2+}$ -dependent action potential. Alternatively, in response to TREK-1 inhibition, the opposing  $\text{Kv}1.4$  and  $\text{Ca}_v3.2$  currents could generate an oscillatory membrane potential resulting in a sustained  $\text{Ca}^{2+}$  influx. Ultimately, the endogenous electrical activity of human AZF cells could be more reliably determined in recordings from intact tissue, such as in an adrenal slice.

In humans, glucocorticoids regulate physiological processes, ranging from energy metabolism to memory consolidation (Stewart and Krone, 2011; Chen et al., 2012). Chronic excessive cortisol secretion as that which occurs in Cushing’s disease or prolonged stress produces systemic as well as central nervous system toxicity, including hippocampal damage and memory impairment (Lupien et al., 1998; Kaouane et al., 2012). Knowledge of human AZF cell ion channels, including their gating and modulation by ACTH and AngII, will be necessary to better

understand the physiology and pathophysiology of cortisol secretion and may be useful in identifying new therapeutic targets to modulate aberrant secretion in disease states.

This work was supported in part by Award Number R56DK047875 (to J. J. Enyeart) from the National Institutes of Health (NIH), National Institute of Diabetes and Digestive and Kidney Diseases (NIDDK) and by the Department of Neuroscience of the Ohio State University Wexner Medical Center. The content is solely the responsibility of the authors and does not necessarily represent the official views of the NIDDK or the NIH.

Lawrence G. Palmer served as editor.

Submitted: 15 January 2013

Accepted: 13 June 2013

## REFERENCES

- Aritomi, S., H. Wagatsuma, T. Numata, Y. Uriu, Y. Nogi, A. Mitsui, T. Konda, Y. Mori, and M. Yoshimura. 2011. Expression of N-type calcium channels in human adrenocortical cells and their contribution to corticosteroid synthesis. *Hypertens. Res.* 34:193–201. <http://dx.doi.org/10.1038/hr.2010.191>
- Armstrong, C.M., and D.R. Matteson. 1985. Two distinct populations of calcium channels in a clonal line of pituitary cells. *Science.* 227:65–67. <http://dx.doi.org/10.1126/science.2578071>
- Augustine, G.J., F. Santamaria, and K. Tanaka. 2003. Local calcium signaling in neurons. *Neuron.* 40:331–346. [http://dx.doi.org/10.1016/S0896-6273\(03\)00639-1](http://dx.doi.org/10.1016/S0896-6273(03)00639-1)
- Bagriantsev, S.N., K.A. Clark, and D.L. Minor Jr. 2012. Metabolic and thermal stimuli control  $\text{K}(2\text{P})2.1$  (TREK-1) through modular sensory and gating domains. *EMBOJ.* 31:3297–3308. <http://dx.doi.org/10.1038/emboj.2012.171>
- Barbara, J.-G., and K. Takeda. 1995. Voltage-dependent currents and modulation of calcium channel expression in zona fasciculata cells from rat adrenal gland. *J. Physiol.* 488:609–622.
- Belluzzi, O., O. Sacchi, and E. Wanke. 1985. A fast transient outward current in the rat sympathetic neurone studied under voltage-clamp conditions. *J. Physiol.* 358:91–108.
- Biagi, B.A., and J.J. Enyeart. 1990. Gadolinium blocks low- and high-threshold calcium currents in pituitary cells. *Am. J. Physiol.* 259:C515–C520.
- Bockenhauer, D., N. Zilberberg, and S.A. Goldstein. 2001. KCNK2: reversible conversion of a hippocampal potassium leak into a voltage-dependent channel. *Nat. Neurosci.* 4:486–491.
- Chen, C.F., and P. Hess. 1990. Mechanism of gating of T-type calcium channels. *J. Gen. Physiol.* 96:603–630. <http://dx.doi.org/10.1085/jgp.96.3.603>
- Chen, D.Y., D. Bambah-Mukku, G. Pollonini, and C.M. Alberini. 2012. Glucocorticoid receptors recruit the  $\text{CaMKII}\alpha$ -BDNF-CREB pathways to mediate memory consolidation. *Nat. Neurosci.* 15: 1707–1714. <http://dx.doi.org/10.1038/nn.3266>
- Choi, M., U.I. Scholl, P. Yue, P. Björklund, B. Zhao, C. Nelson-Williams, W. Ji, Y. Cho, A. Patel, C.J. Men, et al. 2011.  $\text{K}^+$  channel mutations in adrenal aldosterone-producing adenomas and hereditary hypertension. *Science.* 331:768–772. <http://dx.doi.org/10.1126/science.1198785>
- Clark, R.B., W.R. Giles, and Y. Imaizumi. 1988. Properties of the transient outward current in rabbit atrial cells. *J. Physiol.* 405:147–168.
- Clyne, C.D., M.R. Nicol, S. MacDonald, B.C. Williams, and S.W. Walker. 1993. Angiotensin II stimulates growth and steroidogenesis in zona fasciculata/reticularis cells from bovine adrenal cortex via the AT1 receptor subtype. *Endocrinology.* 132:2206–2212. <http://dx.doi.org/10.1210/en.132.5.2206>

- Cooper, E., and A. Shrier. 1989. Inactivation of A currents and A channels on rat nodose neurons in culture. *J. Gen. Physiol.* 94:881–910. <http://dx.doi.org/10.1085/jgp.94.5.881>
- Czirják, G., and P. Enyedi. 2002. TASK-3 dominates the background potassium conductance in rat adrenal glomerulosa cells. *Mol. Endocrinol.* 16:621–629. <http://dx.doi.org/10.1210/me.16.3.621>
- Czirják, G., T. Fischer, A. Spät, F. Lesage, and P. Enyedi. 2000. TASK (TWIK-related acid-sensitive K<sup>+</sup> channel) is expressed in glomerulosa cells of rat adrenal cortex and inhibited by angiotensin II. *Mol. Endocrinol.* 14:863–874. <http://dx.doi.org/10.1210/me.14.6.863>
- Danthi, S., J.A. Enyeart, and J.J. Enyeart. 2003. Modulation of native TREK-1 and Kv1.4 K<sup>+</sup> channels by polyunsaturated fatty acids and lysophospholipids. *J. Membr. Biol.* 195:147–164. <http://dx.doi.org/10.1007/s00232-003-0616-0>
- Danthi, S., J.A. Enyeart, and J.J. Enyeart. 2004. Caffeic acid esters activate TREK-1 potassium channels and inhibit depolarization-dependent secretion. *Mol. Pharmacol.* 65:599–610. <http://dx.doi.org/10.1124/mol.65.3.599>
- Durroux, T., N. Gallo-Payet, and M.D. Payet. 1988. Three components of the calcium current in cultured glomerulosa cells from rat adrenal gland. *J. Physiol.* 404:713–729.
- Enyeart, J.A., L. Xu, and J.J. Enyeart. 2000. A bovine adrenocortical Kv1.4 K<sup>+</sup> channel whose expression is potently inhibited by ACTH. *J. Biol. Chem.* 275:34640–34649. <http://dx.doi.org/10.1074/jbc.M004214200>
- Enyeart, J.A., S.J. Danthi, and J.J. Enyeart. 2003. Corticotropin induces the expression of TREK-1 mRNA and K<sup>+</sup> current in adrenocortical cells. *Mol. Pharmacol.* 64:132–142. <http://dx.doi.org/10.1124/mol.64.1.132>
- Enyeart, J.A., S.J. Danthi, and J.J. Enyeart. 2004. TREK-1 K<sup>+</sup> channels couple angiotensin II receptors to membrane depolarization and aldosterone secretion in bovine adrenal glomerulosa cells. *Am. J. Physiol. Endocrinol. Metab.* 287:E1154–E1165. <http://dx.doi.org/10.1152/ajpendo.00223.2004>
- Enyeart, J.A., H. Liu, and J.J. Enyeart. 2010. cAMP analogs and their metabolites enhance TREK-1 mRNA and K<sup>+</sup> current expression in adrenocortical cells. *Mol. Pharmacol.* 77:469–482. <http://dx.doi.org/10.1124/mol.109.061861>
- Enyeart, J.A., H. Liu, and J.J. Enyeart. 2011. 8-Phenylthio-adenines stimulate the expression of steroid hydroxylases, Cav3.2 Ca<sup>2+</sup> channels, and cortisol synthesis by a cAMP-independent mechanism. *Am. J. Physiol. Endocrinol. Metab.* 301:E941–E954. <http://dx.doi.org/10.1152/ajpendo.00282.2011>
- Enyeart, J.J., B. Mlinar, and J.A. Enyeart. 1993. T-type Ca<sup>2+</sup> channels are required for adrenocorticotropin-stimulated cortisol production by bovine adrenal zona fasciculata cells. *Mol. Endocrinol.* 7:1031–1040. <http://dx.doi.org/10.1210/me.7.8.1031>
- Enyeart, J.J., L. Xu, S. Danthi, and J.A. Enyeart. 2002. An ACTH- and ATP-regulated background K<sup>+</sup> channel in adrenocortical cells is TREK-1. *J. Biol. Chem.* 277:49186–49199. <http://dx.doi.org/10.1074/jbc.M207233200>
- Enyeart, J.J., S.J. Danthi, H. Liu, and J.A. Enyeart. 2005. Angiotensin II inhibits bTREK-1 K<sup>+</sup> channels in adrenocortical cells by separate Ca<sup>2+</sup>- and ATP hydrolysis-dependent mechanisms. *J. Biol. Chem.* 280:30814–30828. <http://dx.doi.org/10.1074/jbc.M504283200>
- Enyeart, J.J., H. Liu, and J.A. Enyeart. 2011. Calcium-dependent inhibition of adrenal TREK-1 channels by angiotensin II and ionomycin. *Am. J. Physiol. Cell Physiol.* 301:C619–C629. <http://dx.doi.org/10.1152/ajpcell.00117.2011>
- Enyedi, P., and G. Czirják. 2010. Molecular background of leak K<sup>+</sup> currents: two-pore domain potassium channels. *Physiol. Rev.* 90:559–605. <http://dx.doi.org/10.1152/physrev.00029.2009>
- Fakler, B., and J.P. Adelman. 2008. Control of K<sub>Ca</sub> channels by calcium nano/microdomains. *Neuron.* 59:873–881. <http://dx.doi.org/10.1016/j.neuron.2008.09.001>
- Ficker, E., and U. Heinemann. 1992. Slow and fast transient potassium currents in cultured rat hippocampal cells. *J. Physiol.* 445:431–455.
- Gomora, J.C., L. Xu, J.A. Enyeart, and J.J. Enyeart. 2000. Effect of mibefradil on voltage-dependent gating and kinetics of T-type Ca<sup>2+</sup> channels in cortisol-secreting cells. *J. Pharmacol. Exp. Ther.* 292:96–103.
- Hamill, O.P., A. Marty, E. Neher, B. Sakmann, and F.J. Sigworth. 1981. Improved patch-clamp techniques for high-resolution current recording from cells and cell-free membrane patches. *Pflügers Arch.* 391:85–100. <http://dx.doi.org/10.1007/BF00656997>
- Hu, C., C.G. Rusin, Z. Tan, N.A. Guagliardo, and P.Q. Barrett. 2012. Zona glomerulosa cells of the mouse adrenal cortex are intrinsic electrical oscillators. *J. Clin. Invest.* 122:2046–2053. <http://dx.doi.org/10.1172/JCI61996>
- Imaizumi, Y., K. Muraki, and M. Watanabe. 1990. Characteristics of transient outward currents in single smooth muscle cells from the ureter of the guinea-pig. *J. Physiol.* 427:301–324.
- Kaouane, N., Y. Porte, M. Vallée, L. Brayda-Bruno, N. Mons, L. Calandreau, A. Marighetto, P.V. Piazza, and A. Desmedt. 2012. Glucocorticoids can induce PTSD-like memory impairments in mice. *Science.* 335:1510–1513. <http://dx.doi.org/10.1126/science.1207615>
- Klöckner, U., J.-H. Lee, L.L. Cribbs, A. Daud, J. Hescheler, A. Pereverzev, E. Perez-Reyes, and T. Schneider. 1999. Comparison of the Ca<sup>2+</sup> currents induced by expression of three cloned  $\alpha$ 1 subunits,  $\alpha$ 1G,  $\alpha$ 1H and  $\alpha$ 1I, of low-voltage-activated T-type Ca<sup>2+</sup> channels. *Eur. J. Neurosci.* 11:4171–4178. <http://dx.doi.org/10.1046/j.1460-9568.1999.00849.x>
- Lansman, J.B. 1990. Blockade of current through single calcium channels by trivalent lanthanide cations. Effect of ionic radius on the rates of ion entry and exit. *J. Gen. Physiol.* 95:679–696. <http://dx.doi.org/10.1085/jgp.95.4.679>
- Lebrethon, M.C., C. Jaillard, G. Defayes, M. Begeot, and J.M. Saez. 1994. Human cultured adrenal fasciculata-reticularis cells are targets for angiotensin-II: effects on cytochrome P450 cholesterol side-chain cleavage, cytochrome P450 17  $\alpha$ -hydroxylase, and 3  $\beta$ -hydroxysteroid-dehydrogenase messenger ribonucleic acid and proteins and on steroidogenic responsiveness to corticotropin and angiotensin-II. *J. Clin. Endocrinol. Metab.* 78:1212–1219. <http://dx.doi.org/10.1210/jc.78.5.1212>
- Lee, J.-H., J.C. Gomora, L.L. Cribbs, and E. Perez-Reyes. 1999. Nickel block of three cloned T-type calcium channels: low concentrations selectively block  $\alpha$ 1H. *Biophys. J.* 77:3034–3042. [http://dx.doi.org/10.1016/S0006-3495\(99\)77134-1](http://dx.doi.org/10.1016/S0006-3495(99)77134-1)
- Lesage, F., C. Terrenoire, G. Romey, and M. Lazdunski. 2000. Human TREK2, a 2P domain mechano-sensitive K<sup>+</sup> channel with multiple regulations by polyunsaturated fatty acids, lysophospholipids, and Gs, Gi, and Gq protein-coupled receptors. *J. Biol. Chem.* 275:28398–28405. <http://dx.doi.org/10.1074/jbc.M002822200>
- Liu, H., J.A. Enyeart, and J.J. Enyeart. 2007. Angiotensin II inhibits native bTREK-1 K<sup>+</sup> channels through a PLC-, kinase C-, and PIP2-independent pathway requiring ATP hydrolysis. *Am. J. Physiol. Cell Physiol.* 293:C682–C695. <http://dx.doi.org/10.1152/ajpcell.00087.2007>
- Liu, H., J.A. Enyeart, and J.J. Enyeart. 2008. ACTH inhibits bTREK-1 K<sup>+</sup> channels through multiple cAMP-dependent signaling pathways. *J. Gen. Physiol.* 132:279–294. <http://dx.doi.org/10.1085/jgp.200810003>
- Liu, H., J.A. Enyeart, and J.J. Enyeart. 2010. ACTH induces Ca<sub>v</sub>3.2 current and mRNA by cAMP-dependent and cAMP-independent mechanisms. *J. Biol. Chem.* 285:20040–20050. <http://dx.doi.org/10.1074/jbc.M110.104190>
- Lupien, S.J., M. de Leon, S. de Santi, A. Convit, C. Tarshish, N.P.V. Nair, M. Thakur, B.S. McEwen, R.L. Hauger, and M.J. Meaney.

1998. Cortisol levels during human aging predict hippocampal atrophy and memory deficits. *Nat. Neurosci.* 1:69–73. <http://dx.doi.org/10.1038/271>
- Lymangrover, J.R., E.K. Matthews, and M. Saffran. 1982. Membrane potential changes of mouse adrenal zona fasciculata cells in response to adrenocorticotropin and adenosine 3',5'-monophosphate. *Endocrinology.* 110:462–468. <http://dx.doi.org/10.1210/endo-110-2-462>
- Matthews, E.K. 1967. Membrane potential measurement in cells of the adrenal gland. *J. Physiol.* 189:139–148.
- Matthews, E.K., and M. Saffran. 1968. Effect of ACTH on the electrical properties of adrenocortical cells. *Nature.* 219:1369–1370. <http://dx.doi.org/10.1038/2191369a0>
- Matthews, E.K., and M. Saffran. 1973. Ionic dependence of adrenal steroidogenesis and ACTH-induced changes in the membrane potential of adrenocortical cells. *J. Physiol.* 234:43–64.
- Mishra, S.K., and K. Hermsmeyer. 1994. Selective inhibition of T-type Ca<sup>2+</sup> channels by Ro 40-5967. *Circ. Res.* 75:144–148. <http://dx.doi.org/10.1161/01.RES.75.1.144>
- Mlinar, B., and J.J. Enyeart. 1993a. Block of current through T-type calcium channels by trivalent metal cations and nickel in neural rat and human cells. *J. Physiol.* 469:639–652.
- Mlinar, B., and J.J. Enyeart. 1993b. Voltage-gated transient currents in bovine adrenal fasciculata cells. II. A-type K<sup>+</sup> current. *J. Gen. Physiol.* 102:239–255. <http://dx.doi.org/10.1085/jgp.102.2.239>
- Mlinar, B., B.A. Biagi, and J.J. Enyeart. 1993a. A novel K<sup>+</sup> current inhibited by adrenocorticotropin hormone and angiotensin II in adrenal cortical cells. *J. Biol. Chem.* 268:8640–8644.
- Mlinar, B., B.A. Biagi, and J.J. Enyeart. 1993b. Voltage-gated transient currents in bovine adrenal fasciculata cells. I. T-type Ca<sup>2+</sup> current. *J. Gen. Physiol.* 102:217–237. <http://dx.doi.org/10.1085/jgp.102.2.217>
- Mlinar, B., B.A. Biagi, and J.J. Enyeart. 1995. Losartan-sensitive AII receptors linked to depolarization-dependent cortisol secretion through a novel signaling pathway. *J. Biol. Chem.* 270:20942–20951. <http://dx.doi.org/10.1074/jbc.270.36.20942>
- Mountjoy, K.G., L.S. Robbins, M.T. Mortrud, and R.D. Cone. 1992. The cloning of a family of genes that encode the melanocortin receptors. *Science.* 257:1248–1251. <http://dx.doi.org/10.1126/science.1325670>
- Natke, E.J. Jr., and E. Kabela. 1979. Electrical responses in cat adrenal cortex: possible relation to aldosterone secretion. *Am. J. Physiol.* 237:E158–E162.
- Omura, M., S. Suematsu, and T. Nishikawa. 2007. Role of calcium messenger systems in ACTH-induced cortisol production in bovine adrenal fasciculo-reticularis cells. *Endocr. J.* 54:585–592. <http://dx.doi.org/10.1507/endocrj.K07-015>
- Payet, M.D., T. Durroux, L. Bilodeau, G. Guillon, and N. Gallo-Payet. 1994. Characterization of K<sup>+</sup> and Ca<sup>2+</sup> ionic currents in glomerulosa cells from human adrenal glands. *Endocrinology.* 134:2589–2598. <http://dx.doi.org/10.1210/en.134.6.2589>
- Perez-Reyes, E. 2003. Molecular physiology of low-voltage-activated t-type calcium channels. *Physiol. Rev.* 83:117–161.
- Perez-Reyes, E., L.L. Cribbs, A. Daud, A.E. Lacerda, J. Barclay, M.P. Williamson, M. Fox, M. Rees, and J.-H. Lee. 1998. Molecular characterization of a neuronal low-voltage-activated T-type calcium channel. *Nature.* 391:896–900. <http://dx.doi.org/10.1038/36110>
- Quinn, S.J., M.C. Cornwall, and G.H. Williams. 1987. Electrical properties of isolated rat adrenal glomerulosa and fasciculata cells. *Endocrinology.* 120:903–914. <http://dx.doi.org/10.1210/endo-120-3-903>
- Segal-Hayoun, Y., A. Cohen, and N. Zilberberg. 2010. Molecular mechanisms underlying membrane-potential-mediated regulation of neuronal K2P2.1 channels. *Mol. Cell. Neurosci.* 43:117–126. <http://dx.doi.org/10.1016/j.mcn.2009.10.002>
- Simpson, E.R., and M.R. Waterman. 1988. Regulation of the synthesis of steroidogenic enzymes in adrenal cortical cells by ACTH. *Annu. Rev. Physiol.* 50:427–440. <http://dx.doi.org/10.1146/annurev.ph.50.030188.002235>
- Stewart, P.M., and N.P. Krone. 2011. The adrenal cortex. In Williams Textbook of Endocrinology. Twelfth edition. S. Melmed, K.S. Polonsky, P.R. Larsen, and H.M. Kronenberg, editors. Saunders Elsevier, Philadelphia. 479–543.
- Tabares, L., J. López-Barneo, and C. de Miguel. 1985. Calcium- and voltage-activated potassium channels in adrenocortical cell membranes. *Biochim. Biophys. Acta.* 814:96–102. [http://dx.doi.org/10.1016/0005-2736\(85\)90423-7](http://dx.doi.org/10.1016/0005-2736(85)90423-7)
- Waterman, M.R. 1994. Biochemical diversity of cAMP-dependent transcription of steroid hydroxylase genes in the adrenal cortex. *J. Biol. Chem.* 269:27783–27786.